Papers

International Journal of Bifurcation and Chaos, Vol. 9, No. 6 (1999) 1009–1039

DIFFERENTIAL EQUATIONS WITH MULTISPIRAL ATTRACTORS

M. A. AZIZ-ALAOUI*
Laboratoire LM, Université du Havre, Faculté des Sciences et Techniques, BP 540, 76058 Le Havre cedex, France

Received July 29, 1998; Revised December 16, 1998

A system of nonautonomous differential equations having Chua's piecewise-linearity is studied. A brief discussion about equilibrium points and their stability is given. It is also extended to obtain a system showing "multispiral" strange attractors, and some of the fundamental routes to "multispiral chaos" and bifurcation phenomena are demonstrated with various examples. The same work is done for other systems of autonomous or nonautonomous differential equations. This is achieved by modifying Chua's piecewise-linearity in order to have additional segments. The evolution of the dynamics and a mechanism for the development of multispiral strange attractors are discussed.

1. Introduction

Many papers have described chaotic systems, one of the most famous being a third-order differential system which models the original Chua circuit [Chua, 1990, 1992, 1993; Madan, 1993]. It contains four linear elements and a nonlinear one (Chua's diode). This nonlinear element is characterized by a piecewise-linear function, characteristic of Chua's resistor whose functional representation is expressed by Eq. (1) below and shown in Fig. 1(a).

In this paper (see also [Aziz-Alaoui, 1997, 1998]), we essentially deal with a nonautonomous dynamical system given by Lacy [1996]. Some other examples of dynamical systems are also studied, each one having Chua's piecewise-linearity (PWL) which is given by:

$$g(v_C) = G_A v_C + \frac{1}{2}(G_B - G_A)[|v_C + B_p| - |v_C - B_p|]\,. \quad (1)$$

The other examples studied are, namely: the Chua system, the Brockett system [Brockett, 1982], the

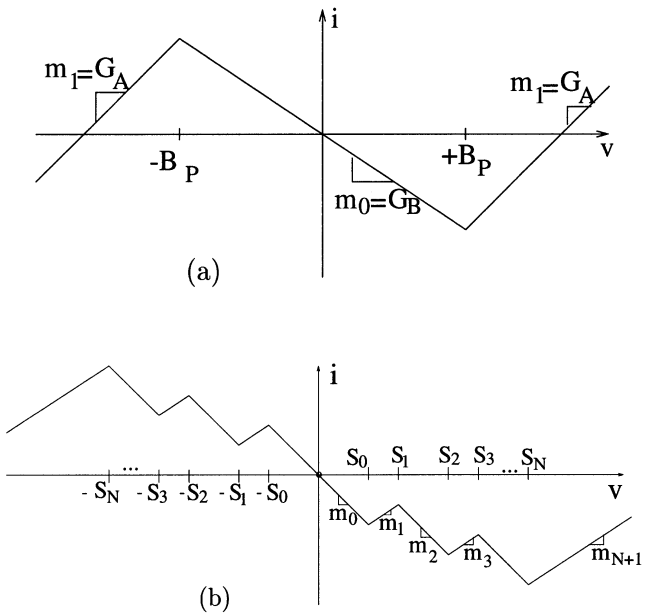

Fig. 1. (a) v–i characteristic of the nonlinear resistor N_R. The slopes of the inner and outer regions are G_B and G_A, respectively, while B_P indicates the breakpoints. (b) The f_N-characteristic of the nonlinear resistor in the multispiral case. $(s_k)_{k\in\mathcal{I}_{N-2}}$ indicate the breakpoints, while $(m_k)_{k\in\mathcal{I}_{N-1}}$ indicate the slopes of the segments.

*E-mail: aziz@fst.univ-lehavre.fr

nonautonomous system given by Reich [1961], and studied by Kapitaniak [1997], and finally the modified van der Pol system [Parker & Chua, 1983; Itoh & Murakami, 1994].

The corresponding dimensionless form of Eq. (1) is given by [Chua, 1992, 1993]:

$$f_2(x) = m_1 x + \frac{1}{2}(m_0 - m_1)[|x+1| - |x-1|]\,. \quad (2)$$

Next, we extend these systems to obtain ones which exhibit various strange attractors with more than two spirals (multispiral attractors). This is achieved by changing the nonlinear resistive element to have one with a modified piecewise-linear characterisitic containing additional segments [see Fig. 1(b)].

Let us remark that multispiral attractors with an even number of spirals (n-double scroll attractors), in Chua's generalized circuit, were first proposed in [Suykens & Vandewalle, 1993]. A more complete family of n-scroll attractors which contains both an even and odd number of spirals was presented in [Suykens *et al.*, 1997] and [Aziz-Alaoui, 1997]. An experimental confirmation of n-double scroll attractors has been presented in [Arena *et al.*, 1996a, 1996b]. Furthermore, using weak linear coupling between chaotic cells, hyperchaos is obtained in a CNN array; this was demonstrated in [Suykens & Chua, 1997] with the n-double scroll hypercube CNN, using n-double scrolls as cells.

To extend the three-segment systems of differential equations to the multispiral case, let us first give the equation for the piecewise-linear function $f_N(.)$ [see Fig. 1(b)]. This "extended" characteristic nonlinear element has additional segments compared to $f_2(.)$, allowing for multispiral strange attractors. It is given by

$$f_N(x) = \begin{cases} m_k x + \operatorname{sgn}(x)\xi_k & \text{if } s_{k-1} \le |x| \le s_k, \\ & \quad k \in \mathcal{I}_{N-2} \\ m_{N-1}x + \operatorname{sgn}(x)\xi_{N-1} & \text{if } |x| \ge s_{N-2}\,, \end{cases} \quad (3)$$

where $N \in \mathbb{N}$, $N \ge 2$, and

- $\mathcal{I}_N = \{0, \ldots, N\}$, $\mathcal{I}_N^* = \{1, \ldots, N\}$;
- $(m_k)_{k\in\mathcal{I}_{N-1}}$ and $(\xi_k)_{k\in\mathcal{I}_{N-1}}$ are two finite and real sequences;
- $(s_k)_{k\in\mathcal{I}_{N-2}}$, is a finite and positive real sequence that is strictly increasing. Furthermore, we will set

$$s_{-1} = 0 \quad \text{and} \quad s_N = +\infty\,. \quad (4)$$

The parameters (m_k), $k \in \mathcal{I}_{N-1}$, are the slopes of f_N in each of the linear segments $[-s_0, s_0]$, $([s_{k-1}, s_k])_{k\in\mathcal{I}_{N-1}^*}$ respectively. Throughout the paper we will assume that

$$\xi_0 = 0 \quad \text{and} \quad s_0 = 1\,. \quad (5)$$

Proposition 1. *The function f_N is continuous if the parameters $(\xi_k)_{k\in\mathcal{I}_{N-1}}$ satisfy:*

$$\begin{gathered} \forall \xi_0 \in \mathbb{R},\ \forall k \in \mathcal{I}_{N-2}^*\,, \\ \xi_{k+1} = (m_k - m_{k+1})s_k + \xi_k\,. \end{gathered} \quad (6)$$

As a result,

$$\begin{gathered} \forall \xi_0 \in \mathbb{R},\ \forall k \in \mathcal{I}_{N-1}^*\,, \\ \xi_k = \xi_0 + \sum_{j=1}^{k} (m_{j-1} - m_j)s_{j-1}\,. \end{gathered} \quad (7)$$

Proof. Obviously, it is sufficient to verify the continuity on the breakpoints $x = s_k$. Let $x > 0$ (otherwise, if $x < 0$, one can give exactly the same proof).

If $x \in [s_{k-1}, s_k]$, $f_N(x) = m_k x + \xi_k$, and if $x \in [s_k, s_{k+1}]$, $f_N(x) = m_{k+1}x + \xi_{k+1}$. Consequently to obtain the continuity of f_N on s_k we only have to verify that

$$\forall\, k \in \mathcal{I}_{N-2}, \quad m_k s_k + \xi_k = m_{k+1}s_k + \xi_{k+1}\,.$$

This last relationship is obviously satisfied if (6) is valid.

On the other hand, formula (7) follows directly by inductive proof from (6). ■

In the following sections we will give the dynamical multispiral systems, i.e. the systems which allow for the emergence of chaotic attractors with N spirals ($N \ge 2$). In addition to some specific parameters, all these systems will also depend on the parameters of the set

$$\mathcal{B}_N = \{(s_k)_{k\in\mathcal{I}_{N-2}}, (m_k)_{k\in\mathcal{I}_{N-1}}\} \subset \mathbb{R}^{2N-1}\,. \quad (8)$$

However, in order to reduce the number of parameters needed to obtain multispiral attractors, the parameters $(m_k)_{k\in\mathcal{I}_{N-1}}$ are chosen to satisfy:

$$m_{2j} = m_0 \quad \text{and} \quad m_{2j+1} = m_1, \quad j = 1, 2, 3\ldots\,, \quad (9)$$

and we will determine the parameters $(s_k)_{k\in\mathcal{I}^*_{N-2}}$ such that the following relationship is satisfied:

$$\mathcal{B}_{2j-2}\subset\mathcal{B}_{2j}\quad\text{and}\quad\mathcal{B}_{2j-1}\subset\mathcal{B}_{2j+1}\,,\qquad j=2,\,3,\,4\ldots\,. \tag{10}$$

We will see that a large number of equilibrium states may exist in such systems (when N increases), and this allows for the emergence of different types of strange attractors, especially multispiral ones. We will also study the transition to chaotic behavior via sequences of period-doubling bifurcations of limit cycles, providing the power spectrum corresponding to the x-component in some cases.

2. A Nonautonomous Chaotic System

2.1. *Introduction and circuit description*

Of all the work done on chaotic systems, the most well-known one is a third-order differential system which models the original Chua circuit. Less work has been done on nonautonomous chaotic systems (see e.g. [Ueda & Akamatsu, 1981; Testa *et al.*, 1982; Murali *et al.*, 1994]). Most of these studies concern second-order systems that incorporate a nonlinear element.

In this section we deal with a simpler circuit than those described in as much as the nonlinear element which is replaced by Chua's piecewise-linearity [Eq. (2)] so that its circuit implementation is amenable to accurate modeling. In [Lacy, 1996] the chaotic behavior of this system was experimentally shown and confirmed by other methods. We give here a dimensionless system of differential equations modeling this circuit, and extend it to obtain a nonautonomous system which shows various strange attractors with more than two spirals. This is achieved by replacing the nonlinear element with one characterized by the function f_N given in Eq. (3), and shown in Fig. 1(b).

The circuit consists of a linear inductor L, a linear resistor R, a linear capacitor C, a periodic voltage source $[V_s\sin(\omega t)]$, and Chua's nonlinear resistor N_R (see Fig. 2).

The equations of the circuit when operating in any of its linear segments are

$$\begin{cases} C\dfrac{dv_C}{d\tau}=i_L-g(v_C)\\[2mm] L\dfrac{di_L}{d\tau}=-Ri_L-i_C+V_S\sin(\omega\tau)\,, \end{cases} \tag{11}$$

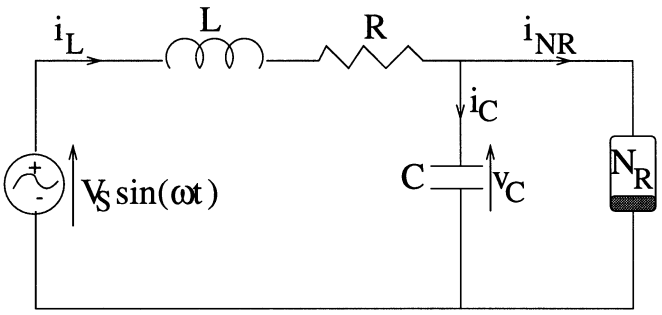

Fig. 2. Electrical schematic diagram of the multispiral nonautonomous circuit.

where $g(.)$ is the piecewise-linear function defined by Eq. (1).

We can transform the state equation (11) into a dimensionless form by rescaling the parameters of the system:

$$x=\frac{v_C}{B_p},\quad y=\frac{i_LR}{B_p},\quad t=\frac{\tau}{RC},$$

$$m_0=G_BB_p,\quad m_1=G_AB_p,\quad \Omega=\frac{\omega}{2\pi RC},$$

$$\alpha=\frac{CR^2}{L},\quad K=\frac{V_S}{B_p}\,.$$

The corresponding dimensionless state equations are then given by

$$\begin{cases} \dfrac{dx}{dt}=y-f_2(x)\\[2mm] \dfrac{dy}{dt}=-\alpha(x+y)+\alpha K\,\sin(2\pi\Omega t)\,, \end{cases} \tag{12}$$

where x and y are functions of t, and f_2 is given by Eq. (2).

2.1.1. *Mathematical study of the multispiral nonautonomous system*

Let us now define the dynamical multispiral nonautonomous system, that is the system which allows for the emergence of chaotic attractors with N spirals:

$$\begin{cases} \dfrac{dx}{dt}=y-f_N(x)\\[2mm] \dfrac{dy}{dt}=-\alpha(x+y)+\alpha K\,\sin(2\pi\Omega t)\,, \end{cases} \tag{13}$$

where f_N is given by Eq. (3).

This system depends on the parameters of the set

$$\mathcal{B}_N^L = \{\alpha,\, K,\, \Omega,\} \cup \mathcal{B}_N \subset \mathbb{R}^{2N+2}\,, \qquad (14)$$

where $\mathcal{B}_N$ is given by Eq. (8). We also assume that Eqs. (4) and (5) are satisfied.

Remark. We can recover the first system (12) by taking $N = 2$, $\xi_0 = 0$ and $s_0 = 1$ (with two spirals at most).

Let D_0 and $D_k^{\pm}(k \in \mathcal{I}_{N-1}^*)$ denote the regions of the x–y plane delimited by the lines $U_{\pm k} = \{(x,\, y),\, x = \pm s_k\}$, $k \in \mathcal{I}_{N-2}$, and let us define $X := (x,\, y)^T$. Then system (13) is equivalent to:

$$\frac{dX}{dt} = MX + F(t,\, X)\,, \qquad (15)$$

where for each region D_0 or $D_k^{\pm}$, $k \in \mathcal{I}_{N-1}^*$, we have

$$M = M_k = \begin{bmatrix} -m_k & 1 \\ -\alpha & -\alpha \end{bmatrix}$$
$$\text{and} \quad F(t,\, X) = F_k(t,\, X) = \begin{pmatrix} -\mathrm{sgn}(x)\xi_k \\ \alpha K\, \sin(2\pi\Omega t) \end{pmatrix}. \qquad (16)$$

Equilibrium points and eigenspaces. Here, we determine the equilibrium points and the eigenspaces corresponding to the homogeneous system derived from (13), i.e. $\dot{X} = M_k X$. In each of the $2N-1$ regions D_0 and $D_k^{\pm}$, $k \in \mathcal{I}_{N-1}^*$, the system is linear and there exists an equilibrium point P_0 or $P_k^{\pm}$, respectively, with $P_k^- = -P_k^+$ due to the symmetry of the vector field [invariance under the transformation $(x,\, y) \to (-x,\, -y)$]. The equilibrium points are given by

$$\begin{cases} P_0 = (0,\, 0)^T \\ P_k^{\pm} = \mp\left(-\dfrac{\xi_k}{1+m_k},\, \dfrac{\xi_k}{1+m_k}\right)^T,\ k \in \mathcal{I}_{N-1}^*\,. \end{cases} \qquad (17)$$

Let us now investigate the stability of the equilibrium points, i.e. the nature of the eigenspaces present in the neighborhood of each $P_k^{\pm}$. As this system is linear in each region $D_k^{\pm}$, the eigenvalues are constant, so that the associated Jacobian matrix M_k is constant and no local approximation is necessary to determine it. This is the essential advantage we obtain from piecewise-linear systems, which nevertheless may exhibit a very complex and rich dynamical behavior.

The characteristic polynomial of the Jacobian matrix M_k is $Q_k = |\lambda_k I - M_k| = \lambda_k^2 + \lambda_k(\alpha + m_k) + \alpha(m_k + 1)$, and the eigenvalues are $\lambda_k^{\pm} = 1/2((\alpha + m_k)^2 \pm \sqrt{\Delta_k})$ where $\Delta_k = (\alpha - m_k)^2 - 4\alpha$.

Based on the value of Δ_k there are two different cases to consider

(i) $\Delta_k \geq 0$: There are two real eigenvalues, so the equilibrium point is a node if $\lambda_k^+ \lambda_k^- > 0$ (stable if $\lambda_k^+ < 0$, unstable if $\lambda_k^+ > 0$), or a saddle point if $\lambda_k^+ \lambda_k^- < 0$.

(ii) $\Delta_k < 0$: There are two complex conjugate eigenvalues: $\lambda_k^{\pm} = r_k \pm j q_k$. If $r_k > 0$ we have an unstable focus. If $r_k < 0$, then we have a stable focus. If $r_k = 0$, then we have a center.

The eigenvectors $V_k^{\pm}$ corresponding to the eigenvalues $\lambda_k^{\pm}$ are determined from the relation $M_k V_k^{\pm} = \lambda_k^+ V_k^{\pm}$, for which the solution is $V_k^{\pm} = (1,\, m_k + \lambda_k^{\pm})^T$. Consequently, in each region D_0 and $D_k^{\pm}$, $k \in \mathcal{I}_{N-1}^*$, the solution of the system $\dot{X} = M_k X$ is

$$\phi_k(t) = c_1(1,\, m_k + \lambda_k^+)^T e^{\lambda_k^+ t} V_k^+ + c_2(1,\, m_k + \lambda_k^-)^T e^{\lambda_k^- t} V_k^-\,, \qquad (18)$$

where c_1 and c_2 are real constants.

The solution of the nonautonomous system $\dot{X} = M_k X + F_k(t,\, x)$ is then

$$\psi_k(t) = e^{(t-t_0)M_k} X(t_0) + e^{tM_k} \int_{t_0}^{t} e^{-sM_k} F_k(s,\, x) ds\,, \qquad (19)$$

where (setting $\Lambda_k^- = m_k + \lambda_k^-$ and $\Lambda_k^+ = m_k + \lambda_k^+$) the matrix e^{tM_k} is given by

$$e^{tM_k} = \frac{1}{\lambda_k^- - \lambda_k^+} \begin{bmatrix} \Lambda_k^- e^{t\lambda_k^+} - \Lambda_k^+ e^{t\lambda_k^-} & e^{t\lambda_k^-} - e^{t\lambda_k^+} \\ \Lambda_k^+ \Lambda_k^- (e^{t\lambda_k^+} - e^{t\lambda_k^-}) & \Lambda_k^- e^{t\lambda_k^-} - \Lambda_k^+ e^{t\lambda_k^+} \end{bmatrix} \qquad (20)$$

and

$$\int_{t_0}^{t} e^{-sM_k} F_k(s,\, x) ds = H_k(t) - H_k(t_0)\,, \qquad (21)$$

where

$$H_k(s) = \begin{pmatrix} e^{-s\lambda_k^+} W_{1,k}^+ - e^{-s\lambda_k^-} W_{1,k}^- \\ e^{-s\lambda_k^+} W_{2,k}^+ - e^{-s\lambda_k^-} W_{2,k}^- \end{pmatrix}, \tag{22}$$

and

$$\begin{cases} W_{1,k}^{\pm} = \operatorname{sgn}(x)\xi_k \dfrac{\Lambda_k^{\mp}}{\lambda_k^{\pm}} + \dfrac{\alpha K}{\lambda_k^{\pm}\left(1 + \left(\dfrac{2\pi\Omega}{\lambda_k^{\pm}}\right)^2\right)} \left[\sin(2\pi\Omega s) + \dfrac{2\pi\Omega}{\lambda_k^{\pm}} \cos(2\pi\Omega s)\right] \\ W_{2,k}^{\pm} = \operatorname{sgn}(x)\xi_k \dfrac{\Lambda_k^{+}\Lambda_k^{-}}{\lambda_k^{\pm}} + \dfrac{\alpha K \Lambda_k^{\pm}}{\lambda_k^{\pm}\left(1 + \left(\dfrac{2\pi\Omega}{\lambda_k^{\pm}}\right)^2\right)} \left[\sin(2\pi\Omega s) + \dfrac{2\pi\Omega}{\lambda_k^{\pm}} \cos(2\pi\Omega s)\right]. \end{cases} \tag{23}$$

With these relations, one can easily study numerical examples of the eigenvalue and eigenspace patterns.

2.2. *Numerical results*

All the phase portrait figures presented in this section are done in the x–y plane. They have been obtained by integrating the systems of differential equations (12) or (13) using the most common fourth-order Runge–Kutta's method. In order to obtain reliable numerical results, the step size has been chosen to be equal to 10^{-4} (or 10^{-5}), and the first 10^7 (or 10^8) steps are discarded to avoid the transient regime. We have employed the same parameters for system (12), namely,

$$\begin{gathered} m_0 = -1.45,\ m_1 = 0.66, \\ \alpha = 0.81,\ \Omega = 0.22\,, \end{gathered} \tag{24}$$

and have used the initial condition

$$X_0 = (-0.1,\, 0.01,\, 0.01)\,. \tag{25}$$

The parameter K was taken as the bifurcation parameter, with values in the interval $[0, 10]$. Furthermore, the parameters m_k, $k \in \mathcal{I}_{N-1}$ are chosen to satisfy Eq. (9), and we will determine the parameters $(s_k)_{k\in\mathcal{I}^*_{N-2}}$ such that the relationship given by Eq. (10) is satisfied.

Formulae (9) and (10) allow us to reduce the number of parameters to determine multispiral attractors. Clearly with the set of parameters $\mathcal{B}_2^L = \{\alpha, K, \Omega, m_0, m_1, s_0\}$ determined [they correspond to system (12) and allow for two-spiral attractors], the new set of parameters allowing four-spiral attractors will be $\mathcal{B}_4^L = \mathcal{B}_2^L \cup \{s_1, s_2\}$, where we only have to look for two new parameters s_1 and s_2, then the new set allowing six-spiral attractors will be $\mathcal{B}_6^L = \mathcal{B}_4^L \cup \{s_3, s_4\}$ and so on.

Figure 3 presents a one-spiral attractor similar to the Rössler–Chua variety.

Figures 4–6 present, respectively, two-, four- and six-spiral strange attractors and the corresponding power spectra, for the sets of parameters $\mathcal{B}_2^L$, $\mathcal{B}_4^L$ and $\mathcal{B}_6^L$ given, respectively, by

$$\begin{cases} N = 2 : \mathcal{B}_2^L = \{\alpha = 0.81,\, K = 1.19,\, \Omega = 0.22, \\ \qquad\qquad m_0 = -1.45,\, m_1 = 0.66\} \\ N = 4 : \mathcal{B}_4^L = \mathcal{B}_2^L \cup \{s_1 = 1.45,\, s_2 = 2.49\} \\ N = 6 : \mathcal{B}_6^L = \mathcal{B}_4^L \cup \{s_3 = 2.94,\, s_4 = 4.1\}\,. \end{cases} \tag{26}$$

The aperiodicity of these attractors can be seen from the calculation of the power spectrum of the time series (here we have chosen the x-component). The power spectrum was calculated for a very long time series using the Cooley–Tukey algorithm [Cooley & Tukey, 1965]. From these figures it seems obvious that the attractor is aperiodic; the spectrum is broadband and contains a dominant discrete peak at a low frequency that is due to the presence of unstable limit cycles (and apparently homoclinic or heteroclinic orbits). We observe that the chaotic attractors evolve around $2N - 1$ steady states. The orbit around the N steady states reveals that the latter might be saddle-foci, whereas the remaining $N - 1$ might be saddle points. These steady states seem to be connected by unstable orbits which are dislocated under the effect of parameter changes. The dominant peak found on the right side of Figs. 4(b), 5(b) and 6(b) corresponds to the fundamental frequency of the sinusoïdal excitation.

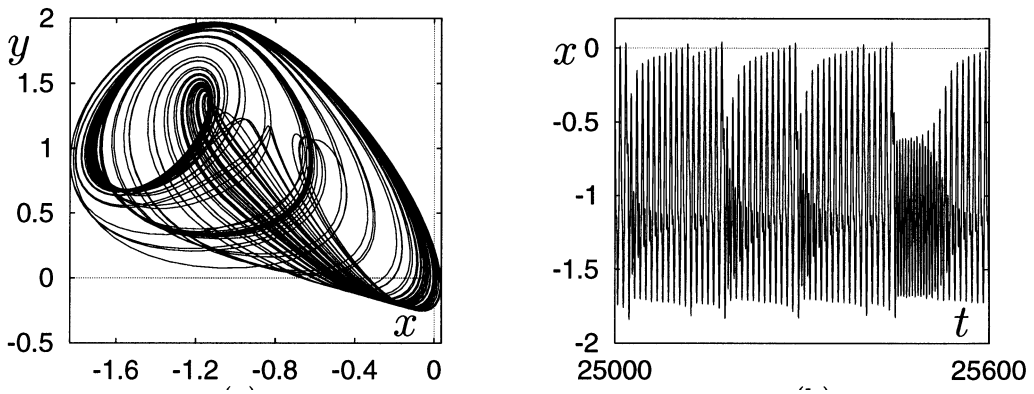

(a) (b)

Fig. 3. (a) Phase portrait in the x–y plane of a one-spiral strange attractor for Eq. (12), $N = 2$, for the set of parameters $\mathcal{B}_2^L$ given by (26) with $K = 1.135$. (b) The time-waveform of the x-component for the same parameters.

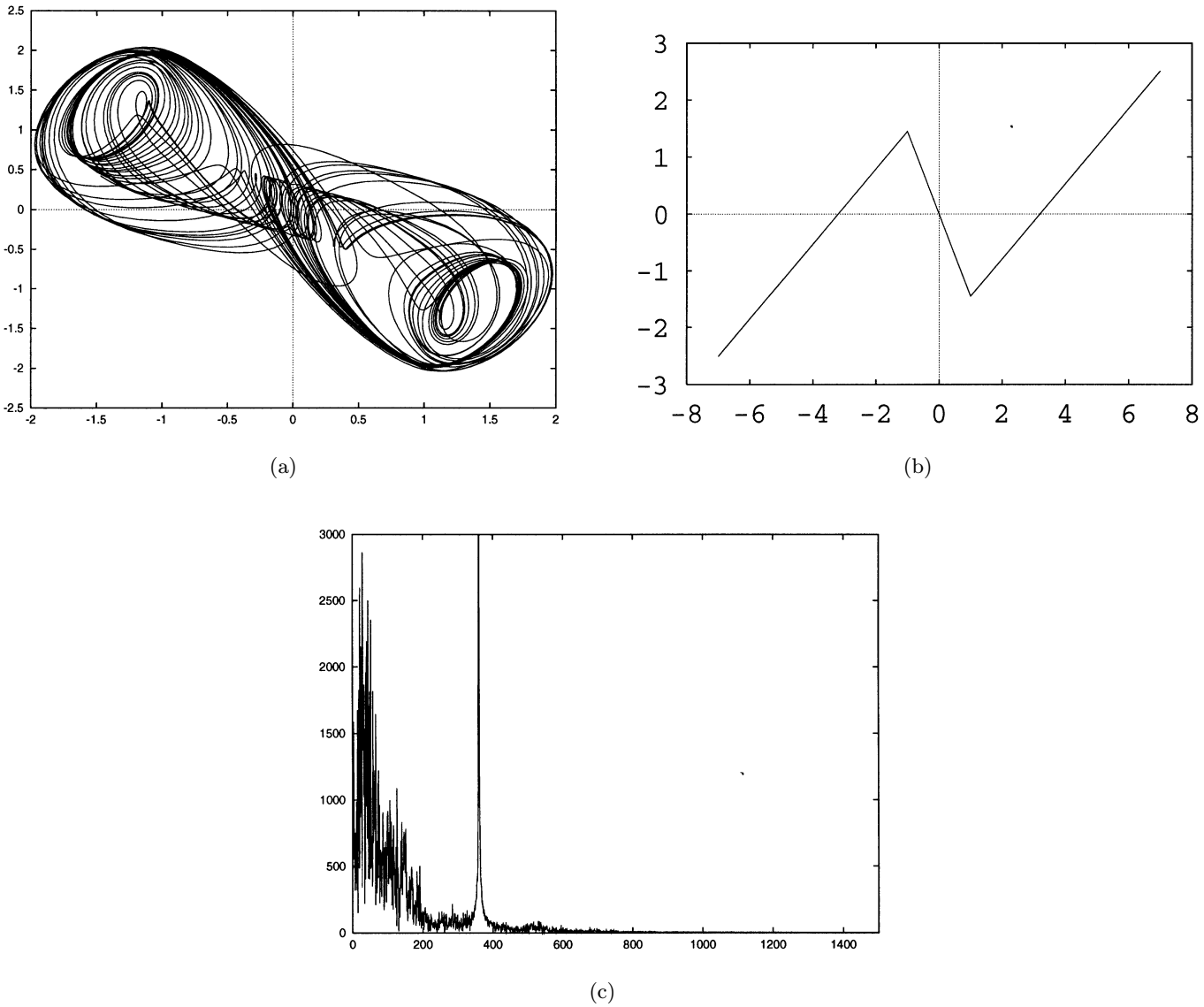

(a) (b) (c)

Fig. 4. (a) Phase portrait in the x–y plane of a strange attractor for Eq. (12), $N = 2$, for the set of parameters $\mathcal{B}_2^L$ given by (26). (b) The corresponding PWL characteristic. (c) The corresponding power spectra of $x(t)$.

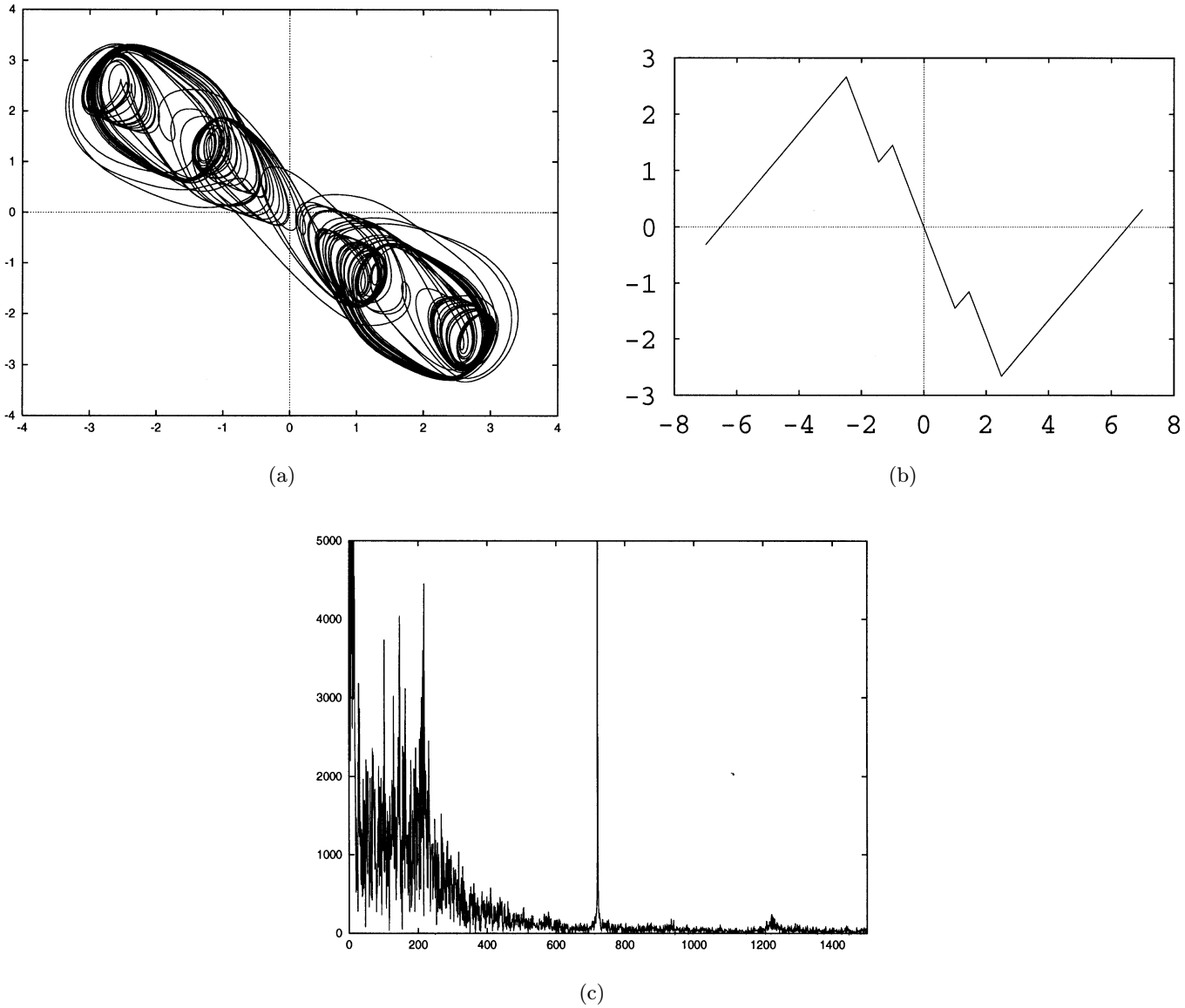

Fig. 5. (a) Phase portrait in the x–y plane of a strange attractor for Eq. (13), $N = 4$, for the set of parameters $\mathcal{B}_4^L$ given by (26). (b) The corresponding PWL characteristic. (c) The corresponding power spectra of $x(t)$.

Figures (7-1)–(7-24) present various phase portraits, illustrating the period-doubling Feigenbaum scenario of the transition chaos or "period-halving", where the parameter K belongs to $[0, 10]$. The figures present an intensive numerical investigation of the behavior of system (13) when N equals 4 and the other parameters are fixed as in (26) (i.e. the set of parameters $\mathcal{B}_4^L$). These investigations are done simultaneously for the initial condition X_0 given by (25) and the associated odd-symmetric initial condition $-X_0$. As K increases from 0 to ∞, there is a very complicated sequence of bifurcations and attractors. In particular, there is a "period-halving" of stable limit cycles as K increases whereby chaos ceases; this is the inverse process of period-doubling.

For $K = 0$ this system is autonomous and has an odd symmetry property, because the equations are then invariant under the transformation $(x, y) \to (-x, -y)$. In that case [Fig. (7-1)], we obtain a stable focus and its symmetric counterpart with respect to $(0, 0)^T$, with formula (18) giving the precise solution. For $K > 0$, formula (19)–(23) give the precise solution in each region D_0 and $D_k^{\pm}$, $(k \in \mathcal{I}_{N-1}^*)$.

For $K \in]0, 7.42]$, stable limit cycles with various periods emerge almost simultaneously for X_0 and $-X_0$, [Figs. (7-2)–(7-4)]. Upon passing through

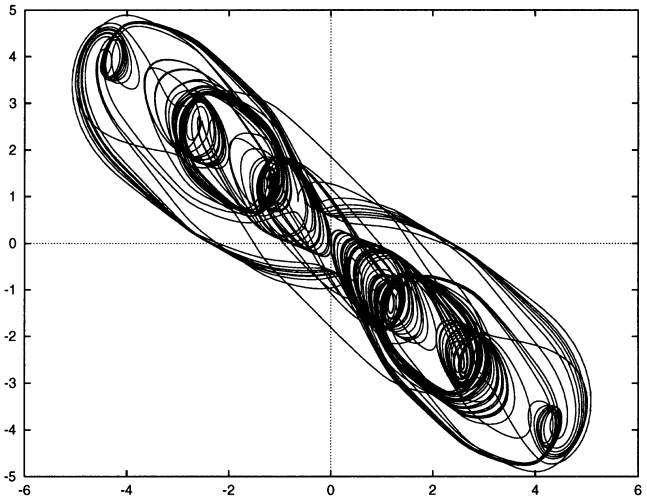

(a)

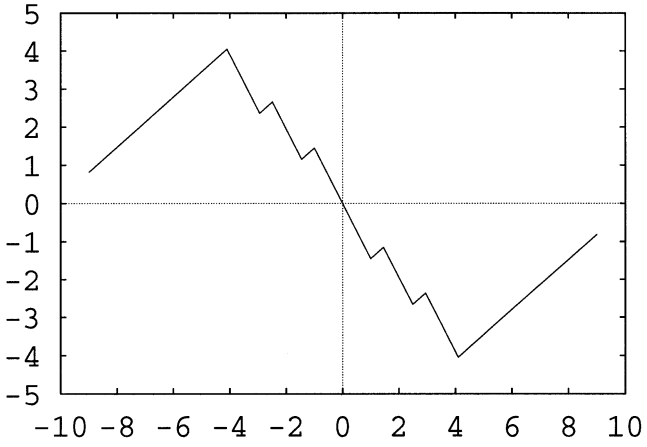

(b)

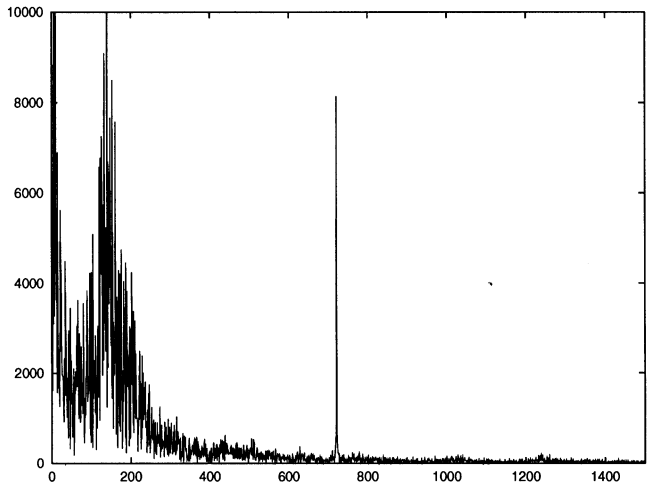

(c)

Fig. 6. (a) Phase portrait in the x–y plane of a strange attractor for Eq. (13), $N = 6$, for the set of parameters $\mathcal{B}_6^L$ given by (26). (b) The corresponding PWL characteristic. (c) The corresponding power spectra of $x(t)$.

the boundary $K = 0.743$ as K increases, sequences of period-doubling bifurcations of various limit cycles give rise to two coexisting chaotic attractors, mostly unsymmetric, showing one spiral first then two spirals, with one corresponding to X_0 the other to $-X_0$ [Figs. (7-5) and (7-6)].

As K increases, these attractors grow in size and are then combined leading to the formation of a four-spiral attractor [Fig. (7-7)]. This chaotic behavior persists up to a threshold of $K = 0.765$ beyond which a quasiperiodic orbit and then a limit cycle of period one reappears. A new area of order is achieved and remains for $K \in [0.765, 1.156]$ [Figs. (7-8)–(7-15)].

The same chaotic scenario starts again for $K \in [1.156, 1.23[$ and new sequences of period-doubling bifurcations occur (always separately for X_0 and $-X_0$) which lead to the almost simultaneous appearence of two-spiral chaotic attractors that grow in size and again give rise to other four-spiral attractors as K increases, [Figs. (7-16)–(7-19)]. This last and unique four-spiral attractor bifurcates to obtain an attractor similar to a three-spiral attractor [Fig. (7-20)]. Finally, upon passing

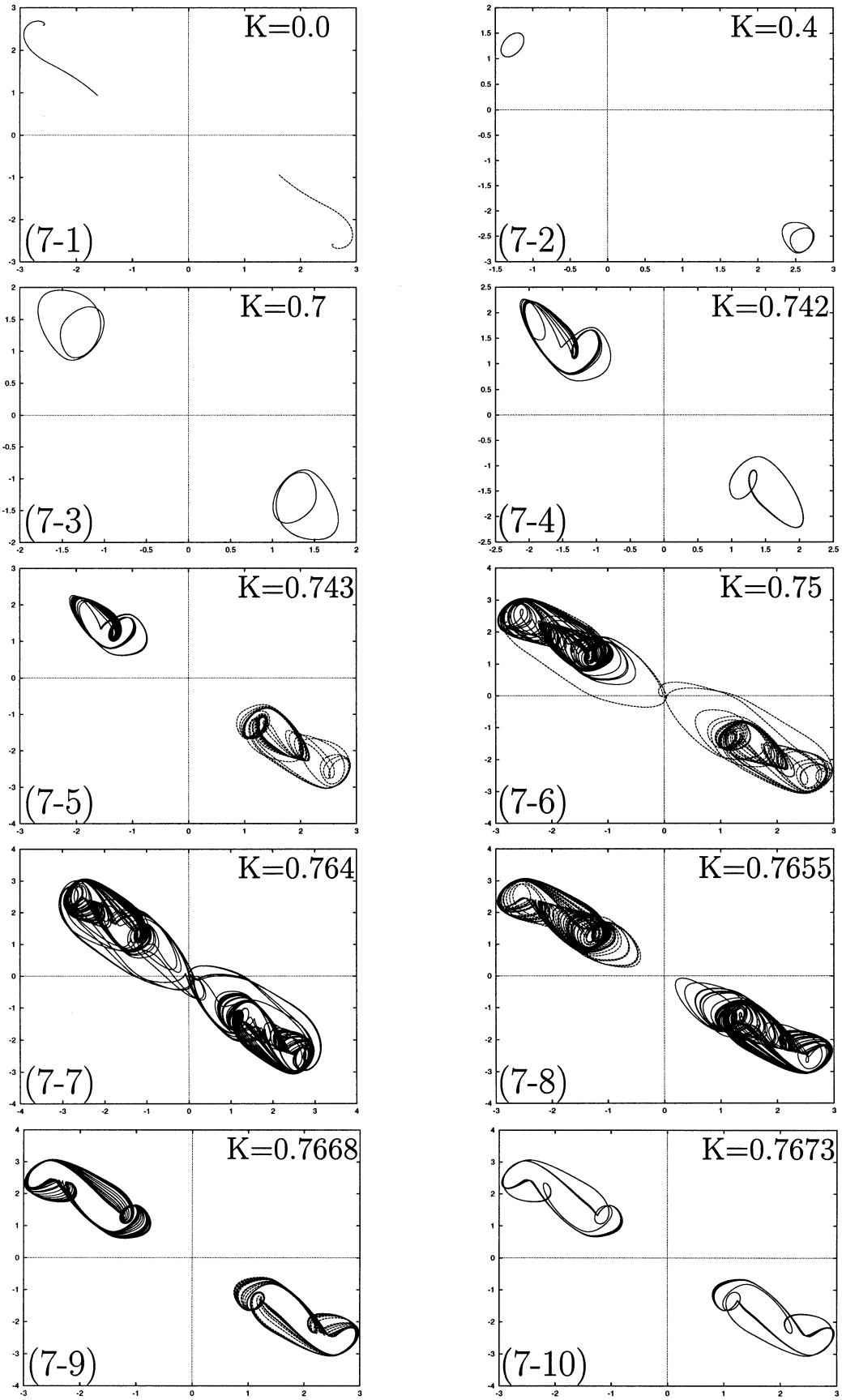

Fig. 7. Transition to chaos via period-doubling from a focus to four-spiral strange attractors (or transition to order via "period-halving") for Eq. (13) with $N = 4$ and for the set of parameters $\mathcal{B}_4^L$ given by (26).

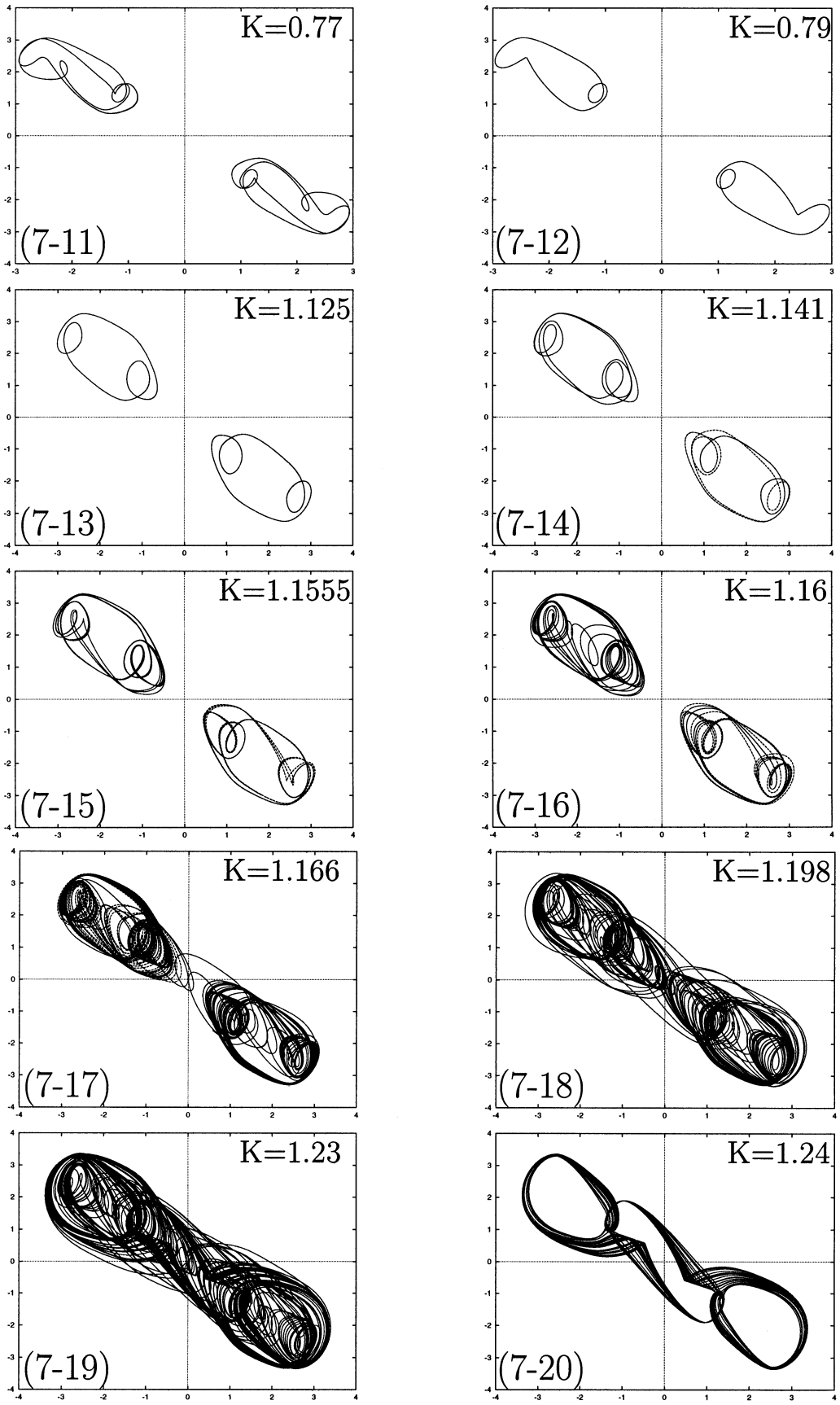

Fig. 7. (*Continued*)

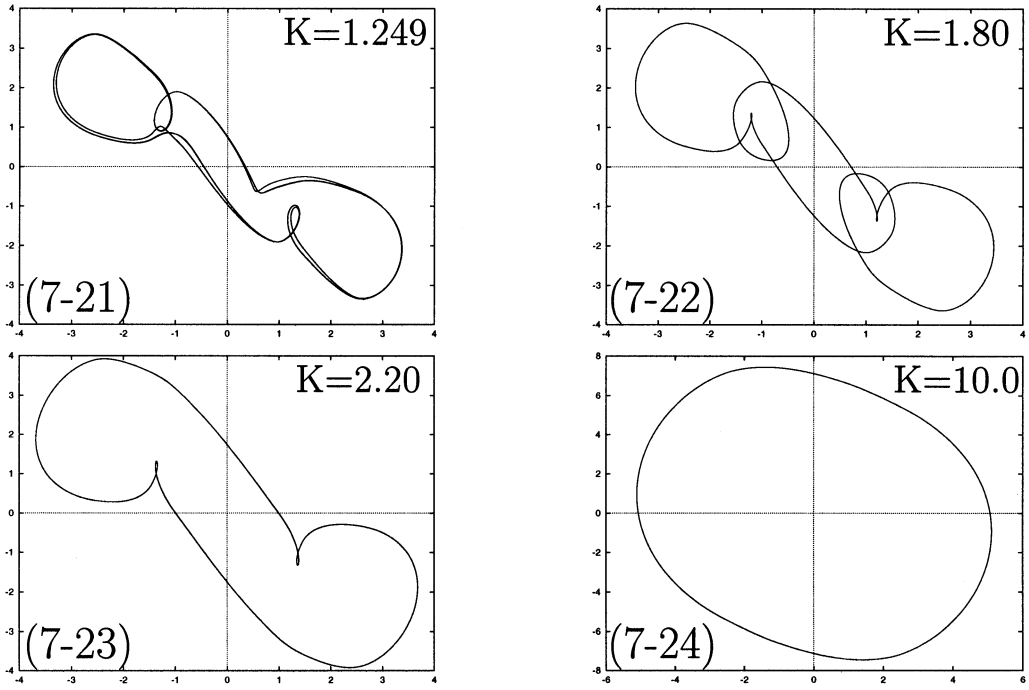

Fig. 7. (*Continued*)

through a critical value of $K = 1.245$, a second and last chaotic area is reached, wherein an "inverse" period-doubling bifurcation of limit cycles leads to a unique limit cycle [Fig. (7-24)], the radius of which goes towards infinity as $K \to +\infty$.

In some cases, the attractors (correponding to X_0 and to $-X_0$) are on the same side of the x–y plane.

3. Chua's Multispiral System

3.1. *Introduction*

In this section, we deal with Chua's system for which the dimensionless state equations are given by

$$\begin{cases} \dfrac{dx}{dt} = \alpha[y - x - f_2(x)] \\ \dfrac{dy}{dt} = x - y + z \\ \dfrac{dz}{dt} = -\beta y - \gamma z\,, \end{cases} \tag{27}$$

where $f_2(.)$ is given by Eq. (2), and x, y and z are functions of t.

To obtain strange chaotic attractors with N spirals, $N \geq 2$, we integrate the differential system

$$\begin{cases} \dfrac{dx}{dt} = \alpha[y - x - f_N(x)] \\ \dfrac{dy}{dt} = x - y + z \\ \dfrac{dz}{dt} = -\beta y - \gamma z\,, \end{cases} \tag{28}$$

where $f_N(.)$ is given by Eq. (3). This system depends on the parameters of the set

$$\mathcal{B}_N^C = \{\alpha, \beta, \gamma\} \cup \mathcal{B}_N \subset \mathbb{R}^{2N+2}\,, \tag{29}$$

where $\mathcal{B}_N$ is given by Eq. (8). We also assume that Eqs. (4) and (5) are satisfied.

Remark. We can recover system (27) from system (28) by taking $N = 2$, $\xi_0 = 0$ and $s_0 = 1$ (with two spirals at most).

Thus the third-order differential system which allows us to obtain three-spiral strange attractors would be given by

$$\begin{cases} \dfrac{dx}{dt} = \alpha[y - x - f_3(x)] \\ \dfrac{dy}{dt} = x - y + z \\ \dfrac{dz}{dt} = -\beta y - \gamma z\,, \end{cases} \tag{30}$$

in which f_3 is defined by

$$f_3(x) = \begin{cases} m_0 x + \mathrm{sgn}(x)\xi_0 & \text{if } |x| \le s_0 \\ m_1 x + \mathrm{sgn}(x)(m_0 - m_1)s_0 & \text{if } s_0 \le |x| \le s_1 \\ m_2 x + \mathrm{sgn}(x)[(m_1 - m_2)s_1 + (m_0 - m_1)s_0] & \text{if } |x| \ge s_1 \end{cases} \tag{31}$$

This system depends on the parameters of the set

$$\mathcal{B}_3^C = \{\alpha, \beta, \gamma\} \cup \mathcal{B}_3 \subset \mathbb{R}^8 , \tag{32}$$

where $\mathcal{B}_3 = \{s_0, s_1, m_0, m_1, m_2\}$. By introducing two new parameters, s_2 and s_3, and replacing f_3 by f_5 in the previous system, one can obtain five-spiral strange attractors with the new set of parameters $\mathcal{B}_5^C = \mathcal{B}_3^C \cup \{s_2, s_3\}$. The next set would be $\mathcal{B}_7^C = \mathcal{B}_5^C \cup \{s_4, s_5\}$, and so on.

Let us define $X := (x, y, z)^T$ and D_0, $D_k^{\pm}(k \in \mathcal{I}_{N-1}^*)$ the regions of $\mathbb{R}^3$ delimited by the planes $\mathcal{U}_{\pm k} = \{(x, y, z),\ x = \pm s_k k \in \mathcal{I}_{N-2}\}$. In each one of these regions, one can write the system (28) as

$$\dot{X} = \mathcal{A}_k X + \mathrm{sgn}(x) U_k , \tag{33}$$

where

$$\mathcal{A}_k = \begin{pmatrix} -\alpha(1 + m_k) & +\alpha & 0 \\ 1 & -1 & 1 \\ 0 & -\beta & -\gamma \end{pmatrix} \quad \text{and} \quad U_k = \begin{pmatrix} -\alpha\xi_k \\ 0 \\ 0 \end{pmatrix} . \tag{34}$$

3.2. *Equilibrium points and eigenspaces*

We will now determine the equilibrium points and the eigenspaces corresponding to system (34).

It is easy to see that in each of the $2N - 1$ regions D_0 and $(D_k)_{k \in \mathcal{I}_{N-1}^*}$, the system is linear and a unique equilibrium point $\mathcal{O}_0$ or $\mathcal{O}_k^{\pm}$ exists, respectively. Due to the symmetry of the vector field i.e. invariance under the transformation $(x, y, z) \to (-x, -y, -z)]$, we have that $\mathcal{O}_k^- = -\mathcal{O}_k^+$. The coordinates of these equilibrium points are

$$\mathcal{O}_k = \left(x_{\mathcal{O}_k}, x_{\mathcal{O}_k} \frac{\gamma}{\beta + \gamma}, x_{\mathcal{O}_k} \frac{-\beta}{\beta + \gamma} \right) , \tag{35}$$

where $$x_{\mathcal{O}_k} = \frac{\xi_k}{\dfrac{\gamma}{\beta + \gamma} - 1 - m_k} .$$

The most interesting cases which can lead to complicated dynamics occur when $[\gamma/(\beta + \gamma)] - 1 - m_k \neq 0$.

Let us now study their stability. As this system is also piecewise-linear in each region D_0 and $(D_k)_{k \in \mathcal{I}_{N-1}^*}$, the eigenvalues are constant so that the associated Jacobian matrix is too and no local approximation is necessary to determine it.

By setting $\Delta_k = 4P_k^3 + 27Q_k^2$, where:

$$P_k = -\frac{A_k^2}{3} + B_k ,$$

$$Q_k = \frac{1}{9}(A_k^3 + A_k^2 - 3A_k B_k + 9C_k) ,$$

$$A_k = (1 + \alpha + \gamma + \alpha m_k) ,$$
$$B_k = \beta + \gamma + \alpha(\gamma + \gamma m_k + m_k) ,$$
$$C_k = \alpha(\beta + \beta m_k + \gamma m_k) ,$$

the eigenvalues of $\mathcal{A}_k$ are the solutions of the cubic equation

$$\Pi(\lambda) = \lambda^3 + A_k\lambda^2 + B_k\lambda + C_k = 0 .$$

Setting $\lambda = \Lambda + \omega$, where $\omega = -(A_k/3)$, we have

$$\Pi(\Lambda) = \Lambda^3 + P_k\Lambda + Q_k .$$

This third-degree polynomial in Λ can be solved using the Cardan formula for each region D_0, $D_k^{\pm}$, $(k \in \mathcal{I}_{N-1}^*)$, resulting in:

(i) If $\Delta_k > 0$, there is a unique real eigenvalue

$$\lambda_k^R = \sqrt[3]{-\frac{Q_k}{2} + \sqrt{\frac{Q_k^2}{4} + \frac{P_k^3}{27}}} + \sqrt[3]{-\frac{Q_k}{2} - \sqrt{\frac{Q_k^2}{4} + \frac{P_k^3}{27}}} - \frac{A_k}{3} , \tag{36}$$

and two complex conjugate eigenvalues

$$(\lambda_k^C)^{\pm} = -\frac{A_k}{3} - \frac{\Lambda_k^R}{2} \pm \frac{j}{2}\sqrt{4P_k + 3(\Lambda_k^R)^2}\,,$$

(ii) If $\Delta_k < 0$, the system has three real and distinct eigenvalues:

$$\lambda_{k,1} = 2\sqrt{-\frac{P_k}{3}}\sin\left(\frac{\theta_k}{3}\right) - \frac{A_k}{3}\,,$$

$$\lambda_{k,2} = 2\sqrt{-\frac{P_k}{3}}\sin\left(\frac{2\pi+\theta_k}{3}\right) - \frac{A_k}{3}\,,$$

and

$$\lambda_{k,3} = 2\sqrt{-\frac{P_k}{3}}\sin\left(\frac{4\pi+\theta_k}{3}\right) - \frac{A_k}{3}$$

where

$$\theta_k = \arcsin\left(\sqrt{\frac{-27Q_k^2}{4P_k^3}}\right) \in [0,\,\pi]\,.$$

The case where $\Delta_k = 0$ corresponds to a measure-zero set of parameters. So by a slight perturbation of parameters and without changing the behavior of the system, a system that belongs to one of the two other cases is obtained.

For the real eigenvalue, the eigenvectors V_k^R satisfy the relation $\mathcal{A}_k V_k^R = \lambda_k^R V_k^R$, $[V_k^R = (v_{k,1},\, v_{k,2},\, v_{k,3})^T]$, so that

$$\begin{cases} -\alpha\left(1+\omega+\dfrac{\lambda_k^R}{\alpha}\right)v_{k,1} + \alpha v_{k,2} = 0 \\ v_{k,1} - (1+\lambda_k^R)v_{k,2} + v_{k,3} = 0 \\ -\beta v_{k,2} - (\gamma+\lambda_k^R)v_{k,3} = 0\,. \end{cases} \tag{37}$$

We easily find that $V_k^R = (1,\,(1/\alpha)(\lambda_k^R + \alpha(1+m_k)),\, (1+\lambda_k^R/\alpha)(\lambda_k^R+\alpha(1+m_k)) - 1)^T$.

For the complex eigenvalues $(\lambda_k^C)^{\pm} = \mu_k \pm i\sigma_k$, the associated eigenspace (two-dimensional) is determined as a linear combination of eigenvectors V_k^1 and V_k^2 such that:

$$\begin{pmatrix} \mathcal{A}-\mu_k I & \sigma_k I \\ \mathcal{A}-\sigma_k I & -\mu_k I \end{pmatrix}\begin{pmatrix} V_k^1 \\ V_k^2 \end{pmatrix} = 0\,.$$

In D_0, if $\Delta_k > 0$ and $s_0 = 1$, $\xi_0 = 0$ (the case for Chua's equations), there exists a basis where the matrix $\mathcal{A}_k$ $(k=0)$ is in the real Jordan form $\mathcal{A}_k = \begin{pmatrix} \lambda_k^R & 0 & 0 \\ 0 & \mu_k & -\sigma_k \\ 0 & \sigma_k & \mu_k \end{pmatrix}$.

The solution of the system is then

$$\begin{cases} x = C_1 e^{\lambda_k^R} \\ y = e^{\mu_k t}(C_2\cos(\sigma_k t) - C_3\sin(\sigma_k t)) \\ z = e^{\mu_k t}(C_4\sin(\sigma_k t) + C_5\cos(\sigma_k t))\,. \end{cases} \tag{38}$$

Therefore the behavior of the system depends on the signs of λ_k^R and μ_k.

3.3. *Numerical results*

As we have done in the previous section, all the phase portraits presented in this section are done in the x–y plane. They have been obtained by integrating the system of differential equations (28) for various values of N using the most common fourth-order Runge–Kutta's method. In order to obtain reliable numerical results, the step size was chosen to be equal to 10^{-4} (or 10^{-5}), and the first 10^7 (or 10^8) steps were discarded to avoid the transient regime. In addition, as in all sections of this paper, we assume that Eqs. (4) and (5) are satisfied.

The initial condition was fixed to be

$$X_0 = (-0.1,\, 0.1,\, 0.1)\,. \tag{39}$$

Furthermore, to obtain an even number of spirals, we have employed the same parameters

$$\alpha = 9.365\,,\quad \beta = 11.79\,,\quad \gamma = 0.04\,. \tag{40}$$

In addition the parameters m_k, $k \in \mathcal{I}_{N-1}$, are chosen to satisfy

$$m_{2j} = m_0 = -\frac{8}{7} \quad\text{and}\quad m_{2j+1} = m_1 = -\frac{5}{7}\,, \qquad j = 1,\,2,\,3,\ldots\,. \tag{41}$$

On the other hand to obtain an odd number of spirals, we have employed the same parameters

$$\alpha = 10.40\,,\quad \beta = 12.5709\,,\quad \gamma = 0.005\,. \tag{42}$$

The parameters m_k, $k \in \mathcal{I}_{N-1}$, are chosen to satisfy

$$m_{2j} = m_0 = -\frac{5}{7} \quad\text{and}\quad m_{2j+1} = m_1 = -\frac{8}{7}\,, \qquad j = 1,\,2,\,3,\ldots\,. \tag{43}$$

In all our numerical tests we have chosen $\xi_0 = 0$ and $s_0 = 1$, as in Sec. 1. The parameter α was taken as the bifurcation parameter.

Finally, we determined the parameters $(s_k)_{k\in\mathcal{I}^*_{N-2}}$ such that the relationship given by Eq. (10) is satisfied. Let us remark that the distinction between the attractors with an even number

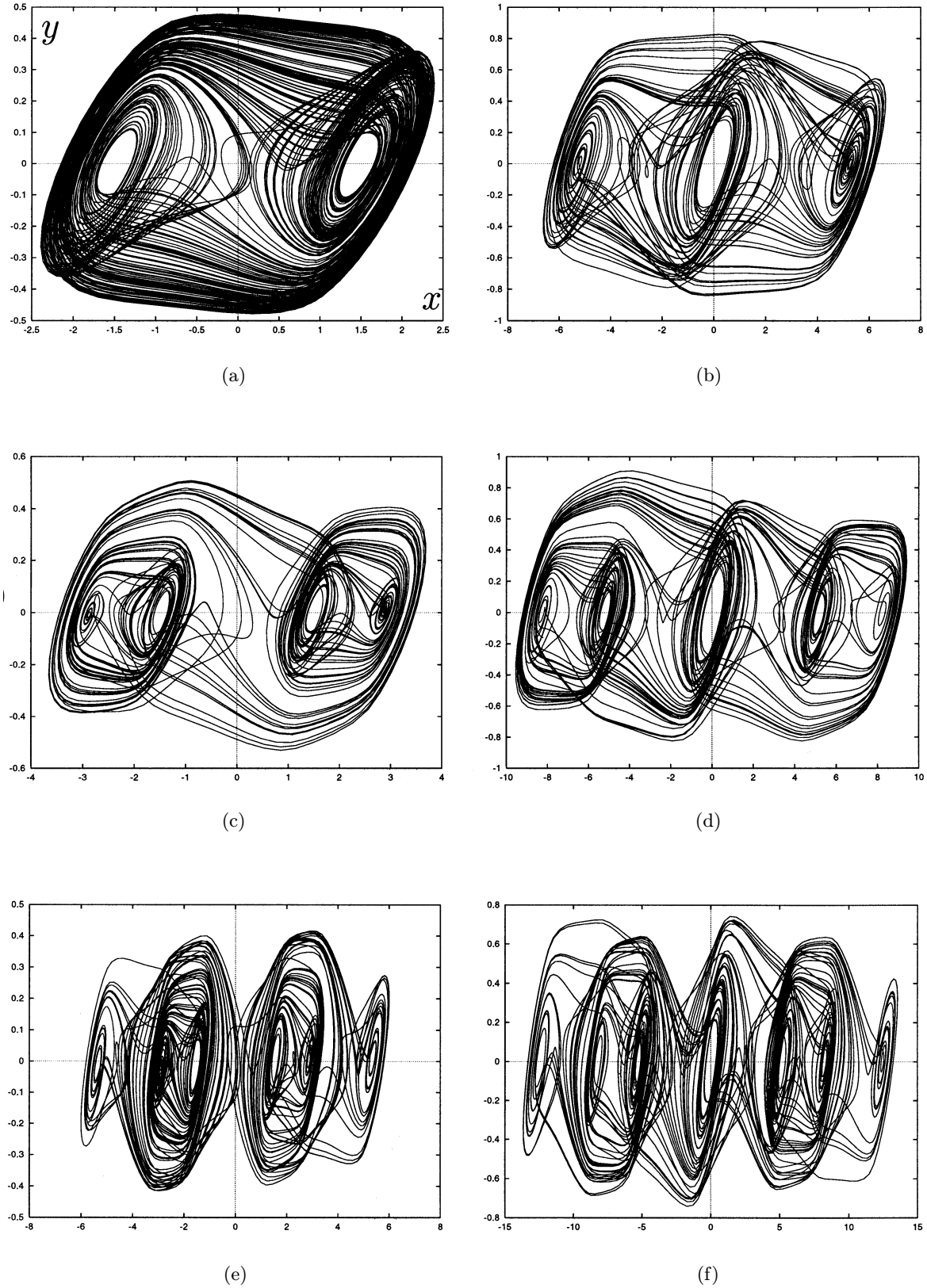

(a) (b)

(c) (d)

(e) (f)

Fig. 8. Phase portraits in the x–y plane of two-, three-, . . . , seven-multispiral attractors corresponding to the set of parameters $\mathcal{B}_N^C$, $N = 2, 3, \ldots, 7$, given by [(44) and (45)], (from upper left, row by row).

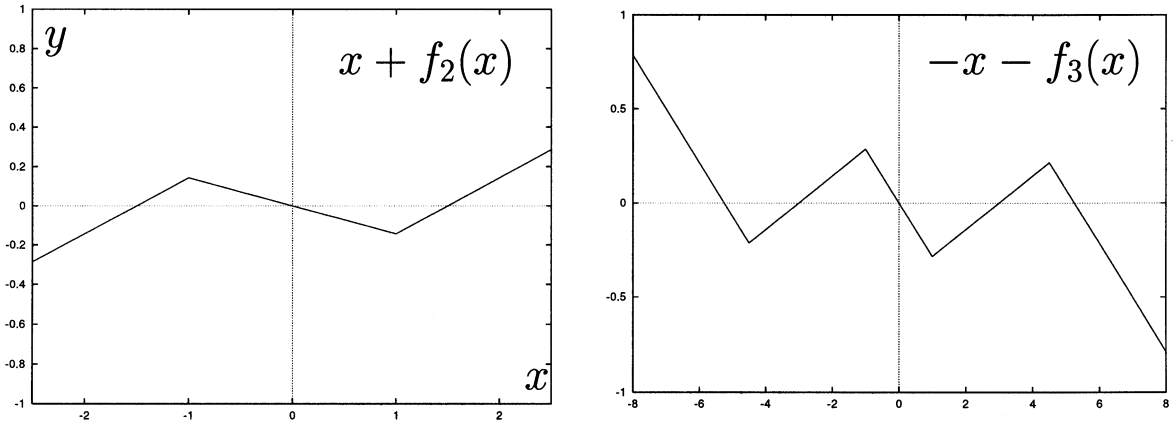

(a′)

(b′)

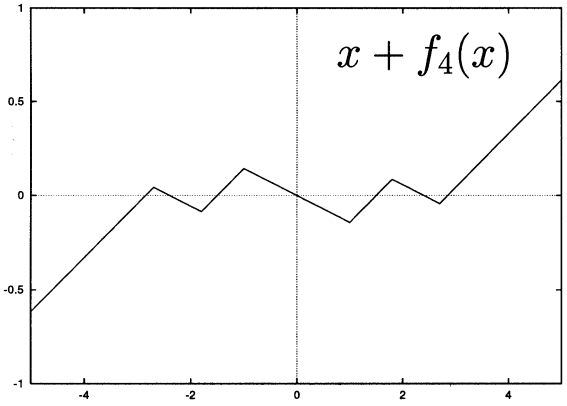

(c′)

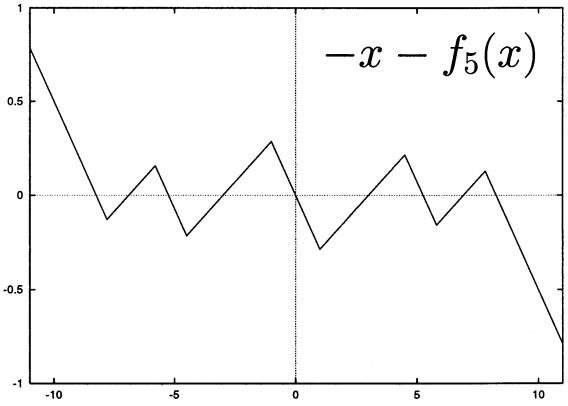

(d′)

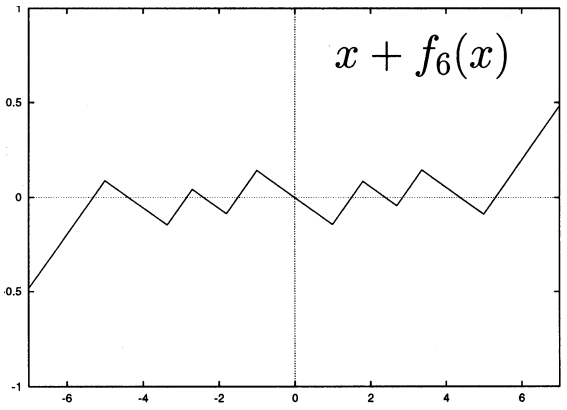

(e′)

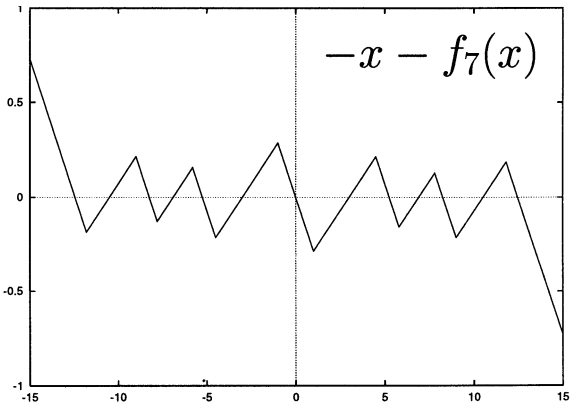

(f′)

Fig. 8. (*Continued*) Nonlinearities $F_N(x)$ corresponding to the PWL f_N allowing the attractors of the previous figure for $N = 2, 3, \ldots, 7$ (from upper left, row by row).

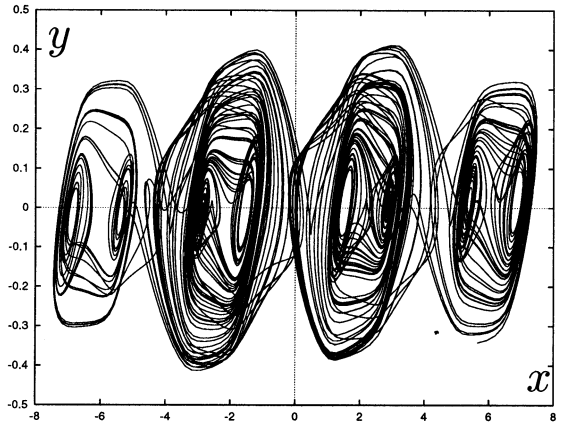

(g)

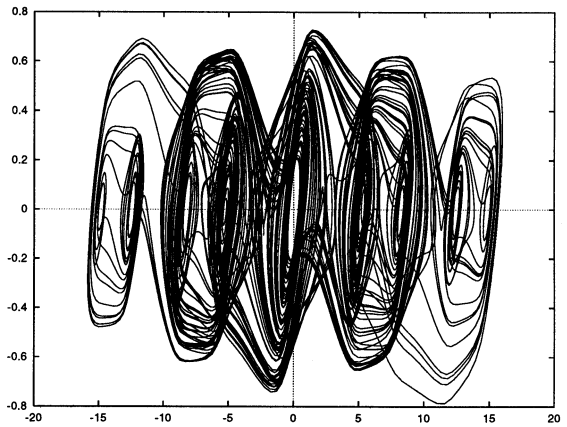

(h)

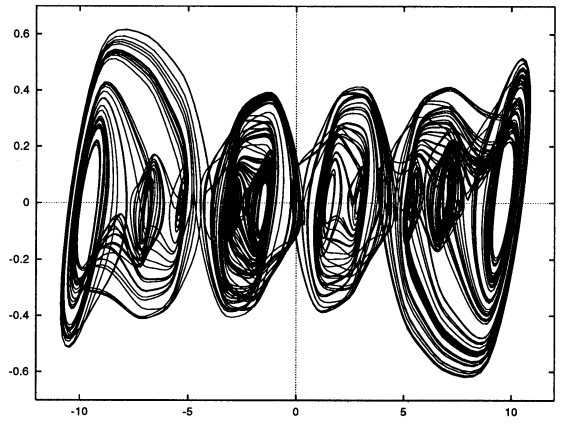

(i)

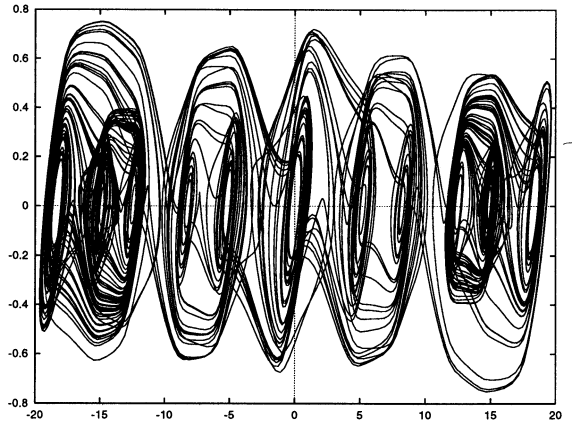

(j)

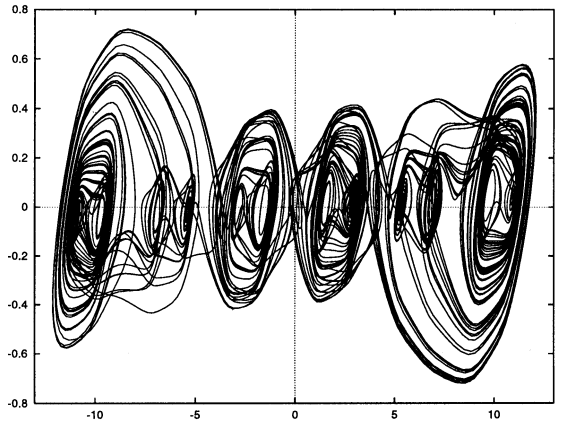

(k)

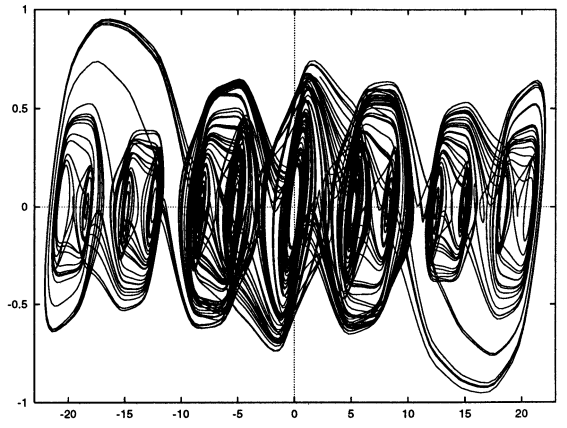

(l)

Fig. 8. (*Continued*) Phase portraits in the x–y plane of multispiral attractors corresponding to sets of parameters $\mathcal{B}_N^C$, $N = 8, 9, \ldots, 13$, given by [(44) and (45)] (from upper left, row by row).

of spirals and an odd number is due to the nature of the equilibrium points that changes when N increases (see Fig. 8). These strange attractors often appear when one-spiral or double-scroll strange attractors (like Chua's one) cling to each other. We give below the parameters used to find the attractors of the following figures:

$$\begin{cases} \text{Fig. 8(a)} : \mathcal{B}_2^C = \{\alpha = 9.365,\ \beta = 11.79, \\ \qquad\qquad \gamma = 0.04,\ s_0 = 1\} \\ \text{Fig. 8(c)} : \mathcal{B}_4^C = \mathcal{B}_2^C \cup \{s_1 = 1.8,\ s_2 = 2.7\} \\ \text{Fig. 8(e)} : \mathcal{B}_6^C = \mathcal{B}_4^C \cup \{s_3 = 3.36,\ s_4 = 5.0\} \\ \text{Fig. 8(g)} : \mathcal{B}_8^C = \mathcal{B}_6^C \cup \{s_5 = 5.6,\ s_6 = 6.6\} \\ \text{Fig. 8(i)} : \mathcal{B}_{10}^C = \mathcal{B}_8^C \cup \{s_7 = 7.15,\ s_8 = 9.0\} \\ \text{Fig. 8(k)} : \mathcal{B}_{12}^C = \mathcal{B}_{10}^C \cup \{s_9 = 9.95,\ s_{10} = 10.75\}\,, \end{cases} \tag{44}$$

$$\begin{cases} \text{Fig. 8(b)} : \mathcal{B}_3^C = \{\alpha = 10.40,\ \beta = 12.5709, \\ \qquad\qquad \gamma = 0.005,\ s_0 = 1,\ s_1 = 4.5\} \\ \text{Fig. 8(d)} : \mathcal{B}_5^C = \mathcal{B}_3^C \cup \{s_2 = 5.8,\ s_3 = 7.8\} \\ \text{Fig. 8(f)} : \mathcal{B}_7^C = \mathcal{B}_5^C \cup \{s_4 = 9.0,\ s_5 = 11.8\} \\ \text{Fig. 8(h)} : \mathcal{B}_9^C = \mathcal{B}_7^C \cup \{s_6 = 12.9,\ s_7 = 14.5\} \\ \text{Fig. 8(j)} : \mathcal{B}_{11}^C = \mathcal{B}_9^C \cup \{s_8 = 15.35,\ s_9 = 17.7\} \\ \text{Fig. 8(l)} : \mathcal{B}_{13}^C = \mathcal{B}_{11}^C \cup \{s_{10} = 18.7,\ s_{11} = 20.2\}\,. \end{cases} \tag{45}$$

Since the plots showing PWL characteristics do not give enough information, we have plotted some corresponding nonlinearities $F_i(x)$ [only for Figs. 8(a)–8(f)]. In this case $F_i(x) = x + f_i(x)$ if i is even and $F_i(x) = -x - f_i(x)$ if i is odd ($i = 2, 3, \ldots, 7$). These nonlinearities give us a more precise idea of the PWL characteristics.

Bifurcations and chaos transition. As the parameter α increases from 0 to ∞ (with β, γ and the other parameters m_k and s_k being fixed), there is a very complicated sequence of bifurcations and attractors. Chaotic and regular oscillatory regimes alternate in a neighborhood of various stable equilibrium states. Processes of period-doubling or inverse period-doubling lead to multispiral strange attractors via the connection of double-scroll strange attractors. Figure 11 gives an impression of the sequence of bifurcations based on numerical calculations, where all the parameters are fixed by the set $\mathcal{B}_8^C$ in Eq. (44), but with α varying. The illustrations are schematic and somewhat simplified.

Figure 12 illustrates this phenomena by presenting examples of trajectories [in the x–y plane] corresponding to these various bifurcations. For the first nine parts of Fig. 12 [Figs. 12(a)–12(i)], we give a trajectory and its symmetric counter part (which always exists because of the odd symmetry

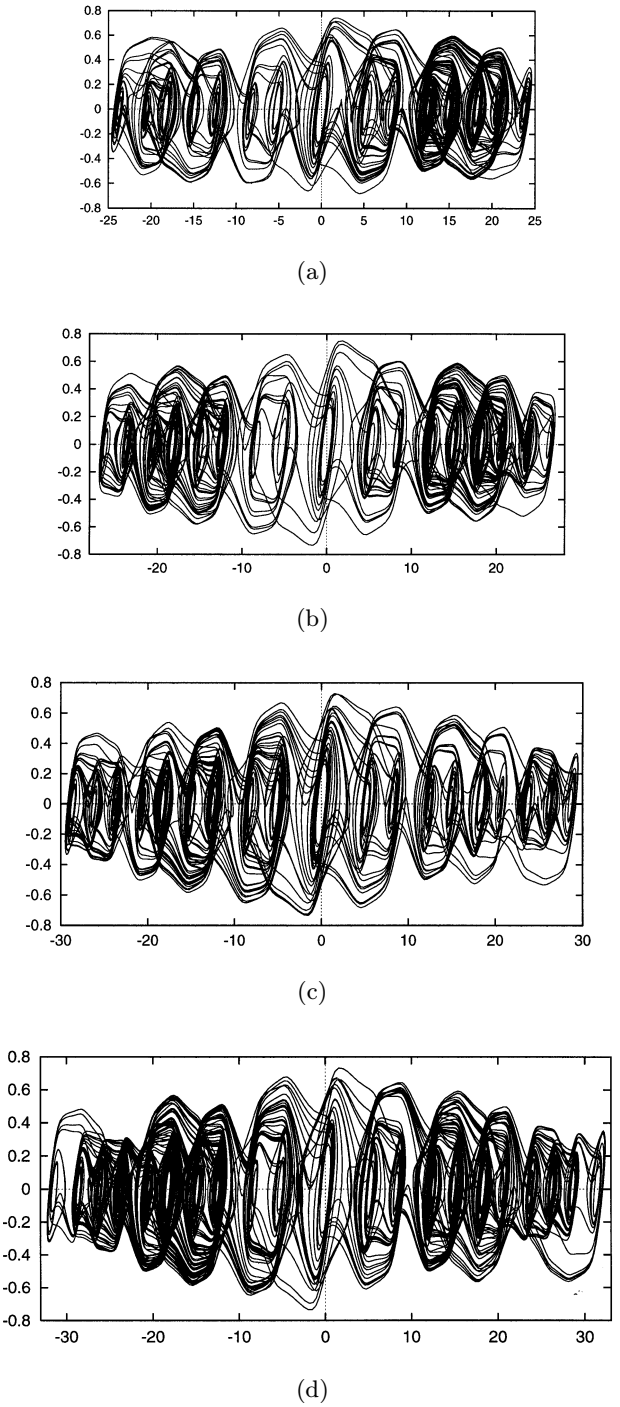

(a) (b) (c) (d)

Fig. 9. 15-, 17-, 19- and 21-spiral strange attractors for the set of parameters specified (a) $\mathcal{B}_{15}^C = \mathcal{B}_{13}^C \cup \{s_{12} = 21.15,\ s_{13} = 23.3\}$, (b) $\mathcal{B}_{17}^C = \mathcal{B}_{15}^C \cup \{s_{14} = 24.2,\ s_{15} = 25.8\}$, (c) $\mathcal{B}_{19}^C = \mathcal{B}_{17}^C \cup \{s_{16} = 26.5,\ s_{17} = 28.2\}$, (d) $\mathcal{B}_{21}^C = \mathcal{B}_{19}^C \cup \{s_{18} = 29.12,\ s_{19} = 31.0\}$, where $\mathcal{B}_{13}^C$ is given by Eq. (45) but with $\alpha = 10.9$ and $s_8 = 15.43$.

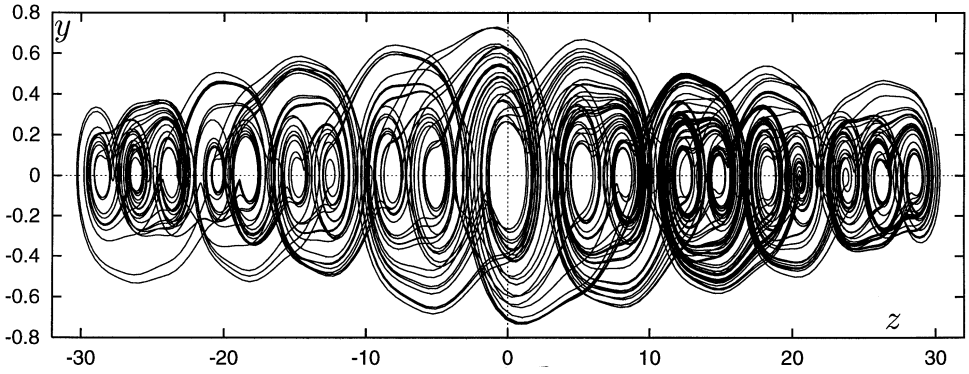

(a)

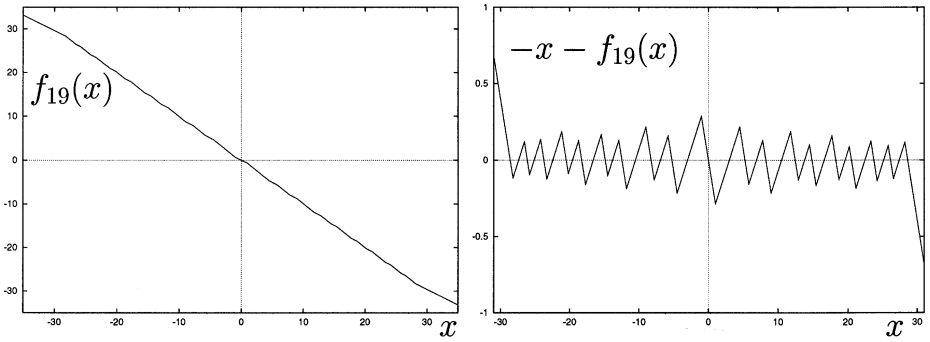

(b) (c)

Fig. 10. (a) The 19-spiral strange attractor given in the previous figure in the z–y plane. (b) PWL $f_{19}(x)$ allowing this attractor, (c) the corresponding nonlinearity $F_{19}(x) = -x - f_{19}(x)$.

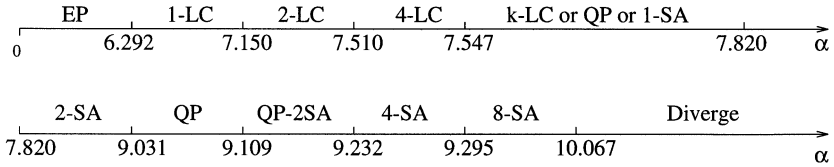

Fig. 11. Symbolic diagram specifying the attractors of system (28) when $N = 8$ (i.e. eight-spiral case) for $\beta = 11.79$, $\gamma = 0.04$ and for the set of parameters $\mathcal{B}_8^C$ given by Eq. (44) with $0 \leq \alpha < \infty$. A stable equilibrium point is denoted by "EP", a stable limit cycle of period k by "k-LC", a strange attractor with k spirals by "k-SA" (a double-scroll is then denoted by "2-SA"), a quasi-periodic trajectory by "QP", and a quasi-periodic trajectory connected with a double-scroll strange attractor by "QP-2SA".

property of the system) while the last two figures [Fig. 12(j) and Fig. 12(k)] present two eight-spiral strange attractors.

Let us remark that the transition via the quasi-periodic trajectory [Fig. 12(g)] is not required to obtain multispiral strange attractors. This depends on the choice of the parameters. It is shown in [Aziz-Alaoui, 1997], that other sets of parameters are possible, and the birth of multispiral attractors is found directly via the connection of two-spiral attractors.

Let us also remark that for a given N one can find strange attractors presenting different shapes (see Fig. 13), or with N' spirals, where $1 \leq N' \leq N$ (see Fig. 14).

$$\begin{cases} \text{Fig. 13.} \\ (a1),(a2),(a3) : \mathcal{B}'_3 = \{\alpha = 14.6,\ \beta = 12.0,\ \gamma = 0.9,\ s_1 = 3,\ m_0 = -\dfrac{5}{7}, \\ \qquad\qquad m_1 = -\dfrac{8}{7},\ m_2 = -0.7\} \\ (b1),(b2),(b3) : \mathcal{B}'_5 = \mathcal{B}'_3 \cup \{s_2 = 4.6,\ s_3 = 5.3,\ m_3 = -1.54,\ m_4 = -0.8\}, \end{cases} \tag{46}$$

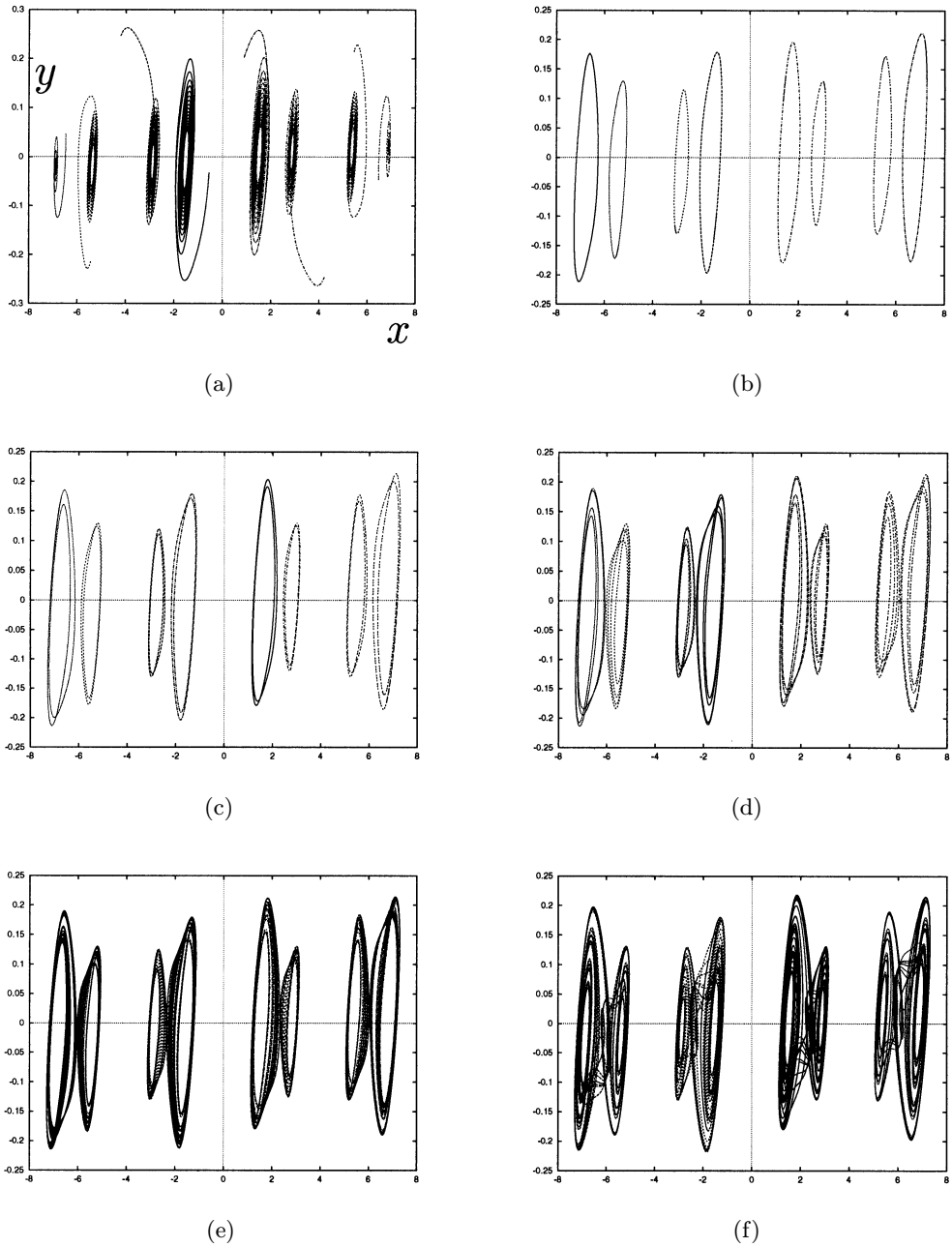

Fig. 12. Phase portraits of *coexisting* attractors for the same parameters and various initial conditions, illustrating the transition to chaos (corresponding to the previous diagram) via period-doubling from a focus to a eight-spiral strange attractor for the set of parameters $\mathcal{B}_8^C$ given by (44). Here α varies and is as specified. (a) $\alpha = 6.0$: stable foci; (b) $\alpha = 7.0$: stable one-limit cycles; (c) $\alpha = 7.35$: stable two-limit cycles; (d) $\alpha = 7.53$: stable four-limit cycles; (e) $\alpha = 7.59$: quasi-periodic trajectories; (f) $\alpha = 7.83$: two-spiral strange attractors; (g) $\alpha = 9.0314$: two quasi-periodic trajectories coexisting with four two-spiral strange attractors; (h) $\alpha = 9.15$: quasi-periodic trajectories connected with two-spiral strange attractors coexisting with two other two-spiral strange attractors; (i) $\alpha = 9.2326$: two coexisting four-spiral strange attractors; (j) $\alpha = 9.35$: an eight-spiral strange attractor; (k) $\alpha = 9.9$: another eight-spiral strange attractor.

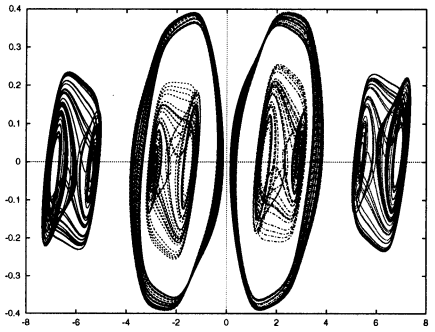

(g)

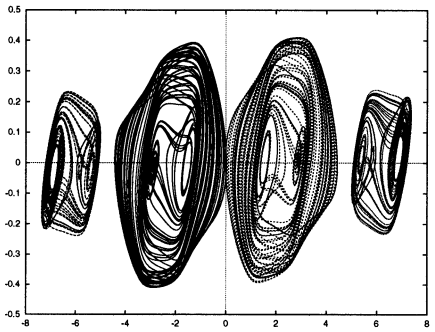

(h)

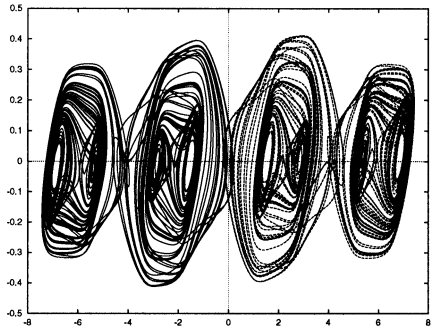

(i)

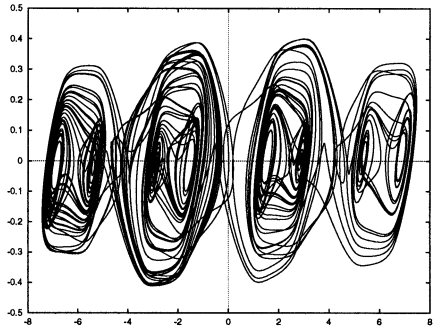

(j)

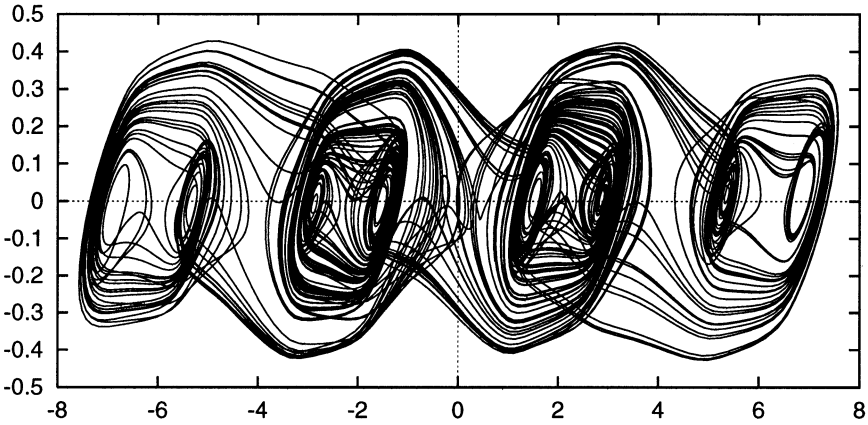

(k)

Fig. 12. (*Continued*)

$$\begin{cases} \text{Fig. 14(a) :} \\ \mathcal{B}_5'' = \{\alpha = 9.7633,\ \beta = 12.5709,\ \gamma = 0.005,\ s_1 = 3,\ s_2 = 5.85,\ s_3 = 6.75, \\ \qquad m_0 = -\dfrac{5}{7}, m_1 = -1.16,\ m_2 = -0.75,\ m_3 = -1.5,\ m_4 = -0.65\}\,, \end{cases} \tag{47}$$

$$\begin{cases} \text{Fig. 14(b) :} \\ \mathcal{B}_7'' = \mathcal{B}_5' \cup \{s_4 = 5.4,\ s_5 = 7.2,\ m_5 = -1.6,\ m_6 = -0.814\}, \\ \text{where } \mathcal{B}_5' \text{ is given by (46)}\,. \end{cases} \tag{48}$$

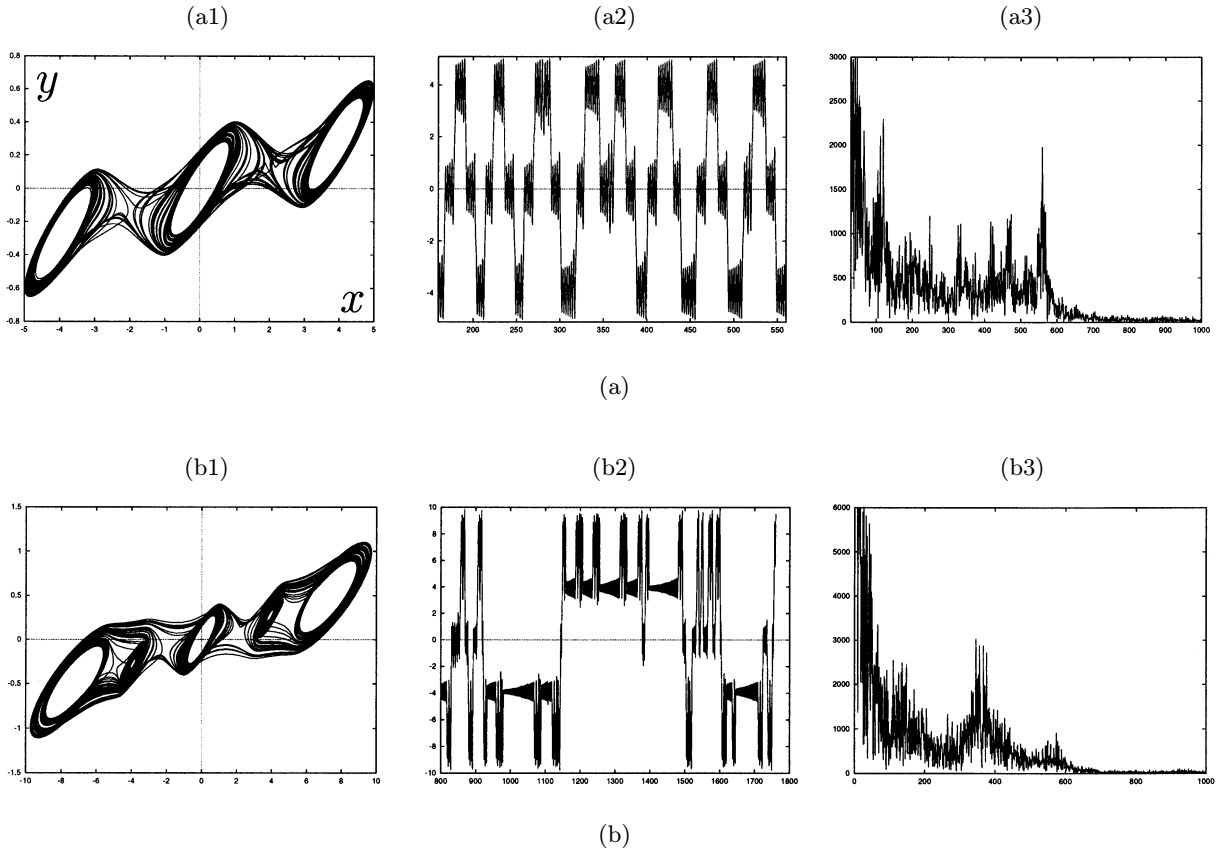

Fig. 13. (a) Three-spiral strange attractor: (a1) projection onto the x–y plane of the phase portrait, (a2) the time waveform of the x-component, (a3) the corresponding power spectra for the set of parameters $\mathcal{B}'_3$ given by (46). (b) Five-spiral strange attractor: (b1) projection onto the x–y plane of the phase portrait, (b2) the time waveform of the x-component, (b3) the corresponding power spectra, for the set of parameters $\mathcal{B}'_5$ given by (46).

4. Brockett's Multispiral System

Brockett [1982] studied the following system:

$$\begin{cases} \dfrac{dx}{dt} = y \\ \dfrac{dy}{dt} = z \\ \dfrac{dz}{dt} = -\beta y - \gamma z + g(x)\,, \end{cases} \tag{49}$$

where the nonlinear function g is given by:

$$g(x) = \begin{cases} -Kx & \text{if } |x| < 1 \\ 2Kx - 3k\,\mathrm{sgn}(x) & \text{if } 1 < |x| < 3 \\ 3K\,\mathrm{sgn}(x) & \text{if } |x| > 3\,. \end{cases} \tag{50}$$

This system exhibits the two-spiral chaotic attractor shown in Fig. 15.

Deregel [1993] remarks that the only interest in region $|x| > 3$ is to claim that all of the solutions of system (49) are bounded when t goes to infinity. This region does not play any role in the dynamics of the system, therefore one can replace the function g by Chua's function f_2 given in Eq. (2). See also [Chua *et al.*, 1993] in which the authors used Chua's oscillator to model other chaotic systems.

If we set

$$m_0 = -K = 1.8 \quad \text{and} \quad m_1 = 2K$$

in the above modified Brockett's system, then for $N = 2$, system (49) presents trajectories qualitatively similar to those in Fig. 15, where explicitly

$$\begin{cases} \dfrac{dx}{dt} = y \\ \dfrac{dy}{dt} = z \\ \dfrac{dy}{dt} = -\beta y - \gamma z + f_N(x)\,. \end{cases} \tag{51}$$

To extend system (49) to obtain Brockett's chaotic attractors with an N-spiral system, we replace the function g by the function f_N given in Eq. (3).

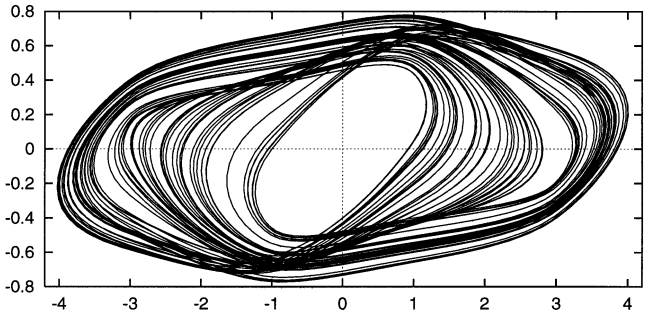

(a)

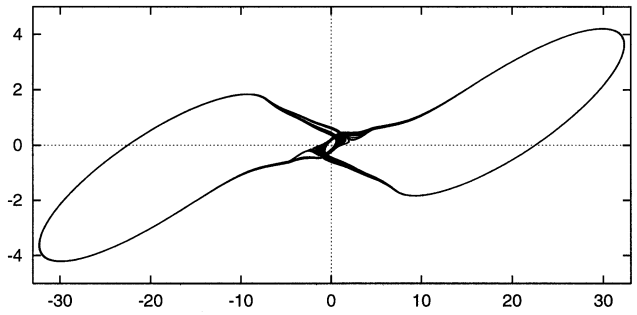

(b)

Fig. 14. Attractors in the x–y plane. (a) for the set of parameters $\mathcal{B}_5''$ given by (47), (b) for the set of parameters $\mathcal{B}_7''$ given by (48).

Hence the new system will depend on the set of the parameters given by

$$\mathcal{B}_N^B = \{\beta,\, \gamma\} \cup \mathcal{B}_N \subset \mathbb{R}^{2N+1}\,, \tag{52}$$

where $\mathcal{B}_N$ is given by Eq. (8). We then adopt the same technique as in the previous sections. Hence we set

$$m_0 = m_{2i} = -K \quad \text{and} \quad m_1 = m_{2i+1} = +2K\,,$$
$$i = 1,\, 2, \ldots\,.$$

After finding a two-spiral attractor, a set of parameters $\mathcal{B}_2^B$ is then determined. To find a four-spiral strange attractor, we look for two new parameters s_1 and s_2 which give a $\mathcal{B}_4^B$ set of parameters ($\mathcal{B}_4^B = \mathcal{B}_2^B \cup \{s_1,\, s_2\}$, and so on).

The following figures (Figs. 16 and 17) show, respectively, four- and six-spiral strange attractors, their corresponding x-component power spectra and their corresponding PWL characteristic. The parameter s_0 is fixed to be equal to 1.0 and the parameter $K = -1.99$. The other parameters are

$$\begin{cases} \text{Fig. 16}: \mathcal{B}_4^B = \{\beta = 1.06,\, \gamma = 0.827, \\ \qquad\qquad\qquad s_1 = 1.65,\, s_2 = 2.1\} \\ \text{Fig. 17}: \mathcal{B}_6^B = \mathcal{B}_4^B \cup \{s_3 = 2.5,\, s_4 = 4.1\}\,. \end{cases} \tag{53}$$

5. Multispiral Chaotic and Nonchaotic Attractors in a Quasi-Periodically Forced System

Kapitaniak [1997] has shown that aperiodic nonchaotic trajectory characteristic of strange nonchaotic attractors can occur on a two-frequency torus. He investigated the dynamics of the nonautonomous circuit which is a classical configuration of a forced negative-resistance oscillator [Reich, 1961]. (Concerning nonchaotic strange attractors, see, e.g. [Brindley & Kapitaniak, 1991; Grebogi *et al.*, 1984; Ding *et al.*, 1989] and references cited therein.) The dynamics of the circuit considered is described by the following dimensionless equations:

$$\begin{cases} \dfrac{dx}{dt} = y - f_2(x) \\ \dfrac{dy}{dt} = -\beta[x + (v+1)y) + A(\sin(\omega_1 t) + \sin(\omega_2 t)]\,, \end{cases} \tag{54}$$

where f_2 is the nonlinear piecewise-linear function given by Eq. (2). The dynamics of Eq. (54) depends on the parameters β, v, m_0, m_1, ω_1, ω_2, and the amplitude A.

Here we consider the extension of system (54) to a system allowing multispiral nonchaotic or chaotic attractors. We replace the function f_2 by the function f_N given in Eq. (3) and, as in the previous sections, we also assume that Eqs. (4) and (5) are satisfied. Hence, the new system will be:

$$\begin{cases} \dfrac{dx}{dt} = y - f_N(x) \\ \dfrac{dy}{dt} = -\beta[x + (v+1)y) + A(\sin(\omega_1 t) + \sin(\omega_2 t)]\,. \end{cases} \tag{55}$$

It depends on the set of parameters:

$$\mathcal{B}_N^K = \{\beta,\, v,\, \omega_1,\, \omega_2,\, A\} \cup \mathcal{B}_N \subset \mathbb{R}^{2N+4}\,, \tag{56}$$

where $\mathcal{B}_N$ is given by Eq. (8). For our numerical results we set (as in [Kapitaniak, 1997])

$$\beta = 1.0,\ v = 0.015,\ \omega_1 = 0.75,\ \omega_2 = \sqrt{2}\,. \tag{57}$$

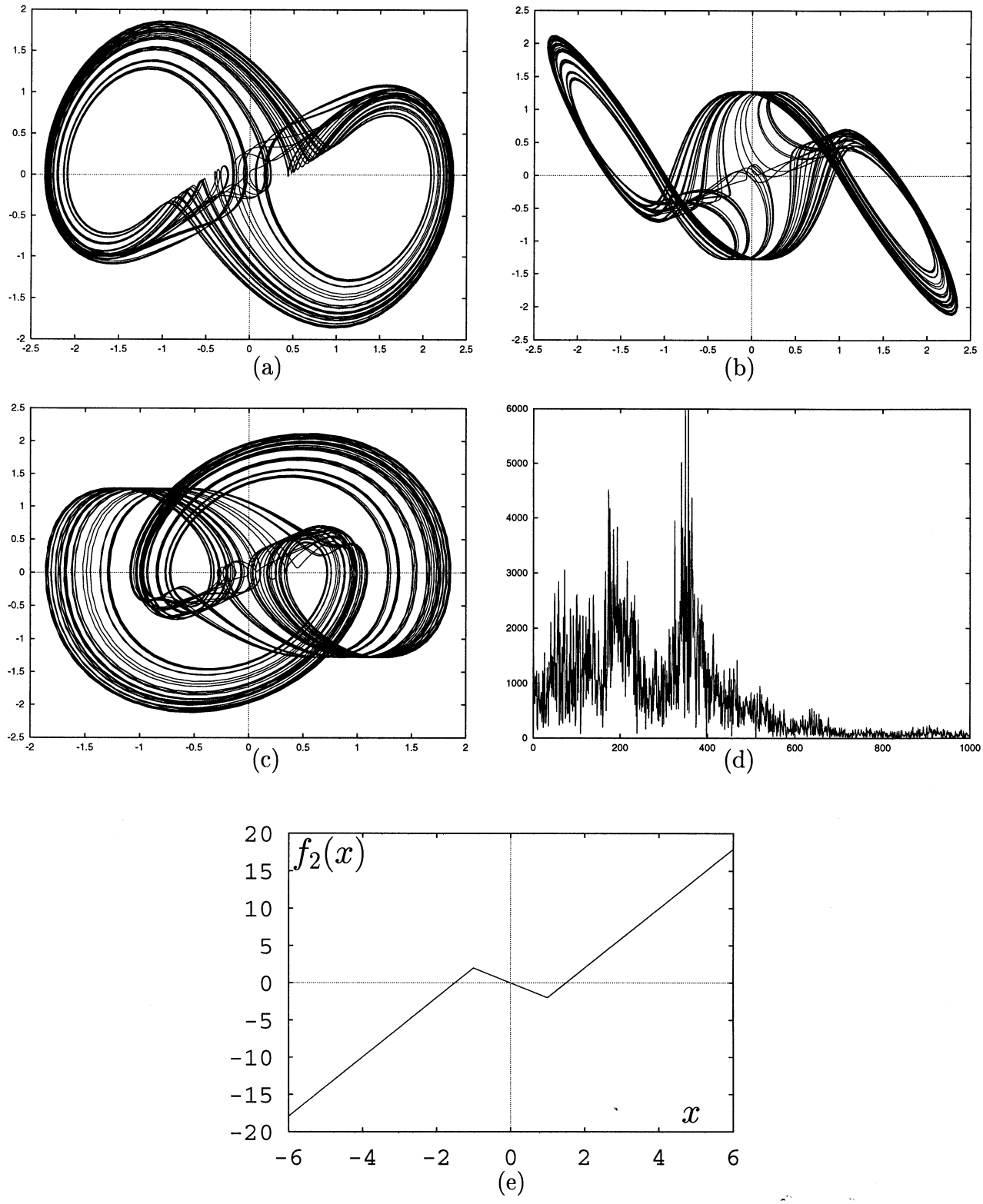

Fig. 15. Phase portrait of the modified Brockett system (51) for $N = 2$ and for $\mathcal{B} = 1.25$ $\gamma = 1.0$, $m_0 = 1.8$ and $m_1 = -2m_0$. (a) In the x–y plane. (b) In the x–z plane. (c) In the y–z plane. (d) The power spectra of the x-component. (e) The actual PWL characteristic, f_2, corresponding to this attractor.

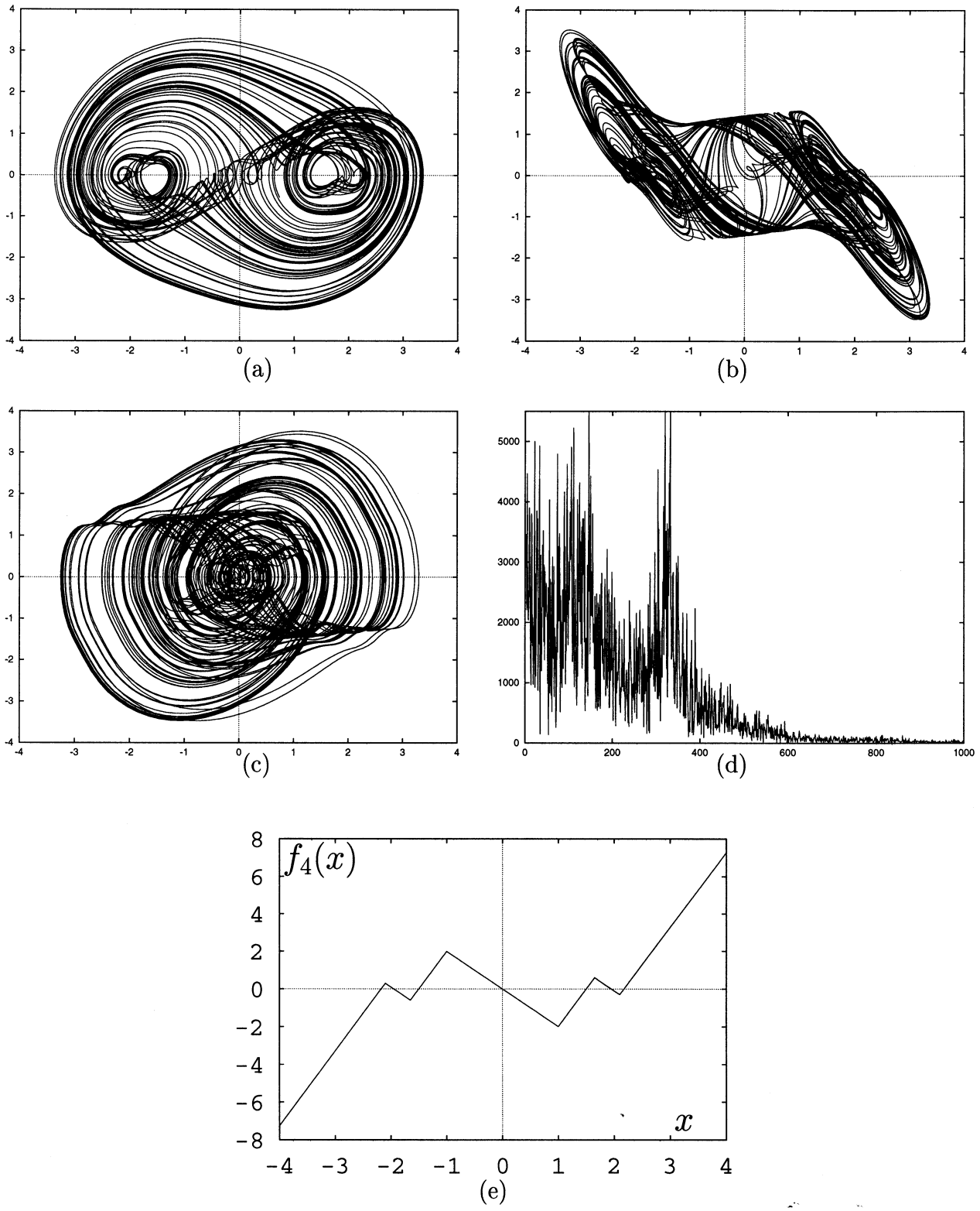

Fig. 16. Phase portrait of the modified Brockett system for $N = 4$ and for $\mathcal{B}_4^B$ given by Eq. (53), with $K = -1.99$. (a) In the x–y plane. (b) In the x–z plane. (c) In the y–z plane. (d) The power spectra of the x-component. (e) The actual PWL characteristic, f_4, corresponding to this four-spiral attractor.

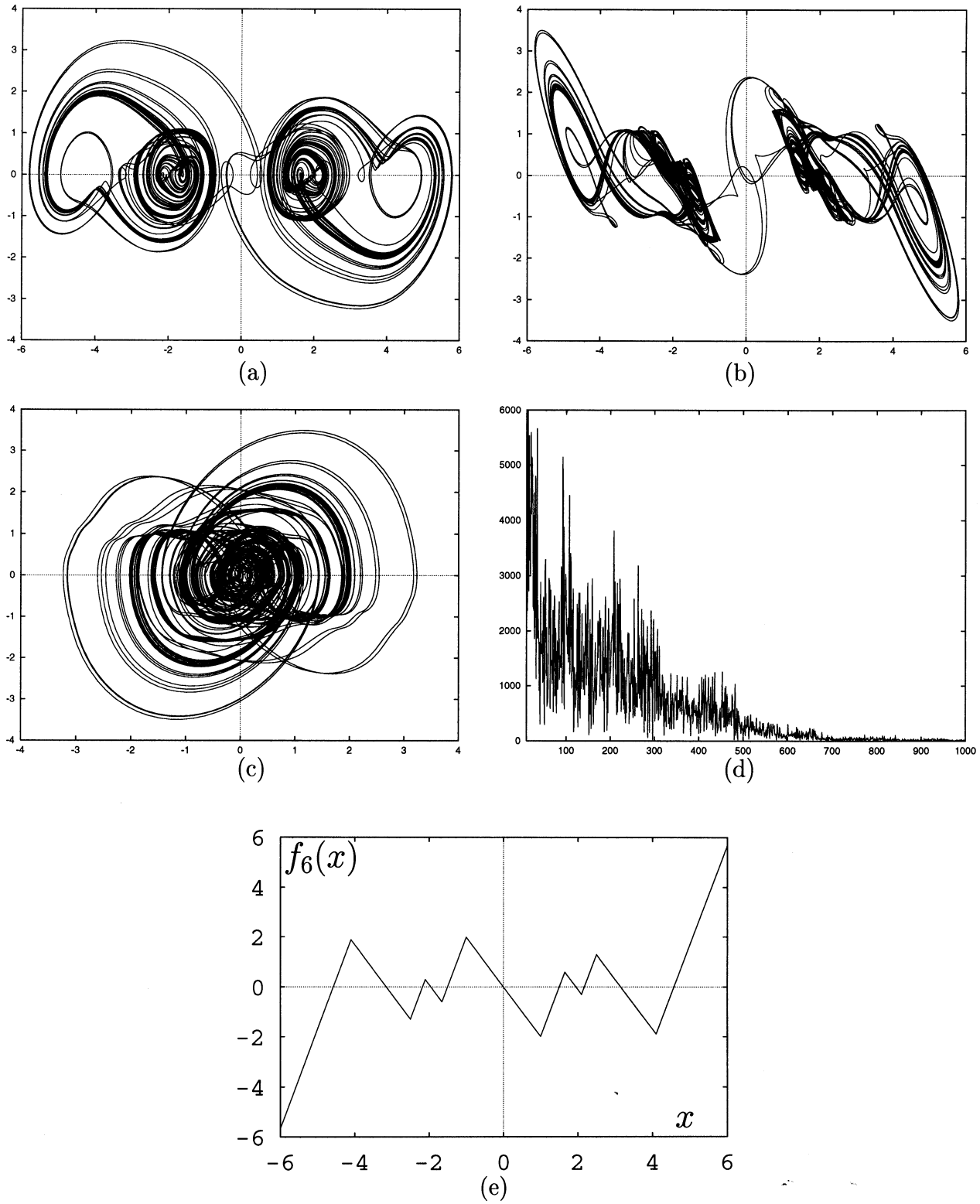

Fig. 17. Phase portraits of the modified Brockett system for $N = 6$ and for $\mathcal{B}_6^B$ given by Eq. (53), with $K = -1.99$, $s_3 = 2.5$ and $s_4 = 4.1$. (a) In the x–y plane. (b) In the x–z plane. (c) In the y–z plane. (d) The power spectra of the x-component. (e) The actual PWL characteristic, f_6, corresponding to this attractor.

We also set

$$m_0 = m_{2i} = \cdots = -1.02$$
$$\text{and } m_1 = m_{2i+1} = \cdots = -0.55\,,\ i = 1, 2, \ldots\,. \tag{58}$$

Therefore, the parameters used to obtain Figs. 18–21 below are given by

$$\begin{cases} \mathcal{B}_2^K = \mathcal{B}_2 \cup \{A\}\,, \\ \text{where} \\ \mathcal{B}_2 = \{\beta = 1.0,\ v = 0.015,\ \omega_1 = 0.75,\ \omega_2 = \sqrt{2}, \\ \qquad m_0 = -1.02,\ m_1 = -0.55,\ s_0 = 1.0\}\,. \end{cases} \tag{59}$$

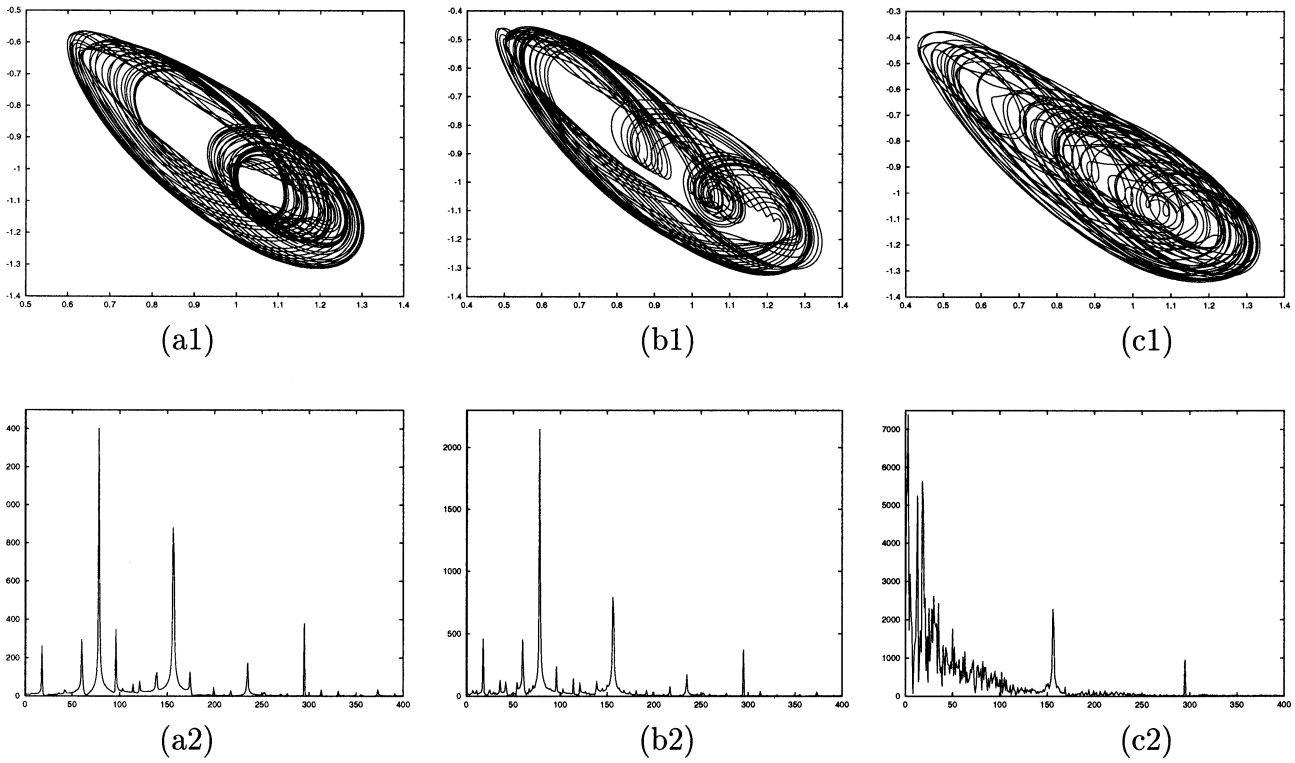

Fig. 18. Attractors and the corresponding x-component power spectra for system (55) with $N = 2$ and the set of parameters $\mathcal{B}_2^K$ given by (60). (a1,2) two-frequency torus for $A = 0.08$; (b1,2) two-frequency torus for $A = 0.088$; (c1,2) strange chaotic attractor for $A = 0.092$.

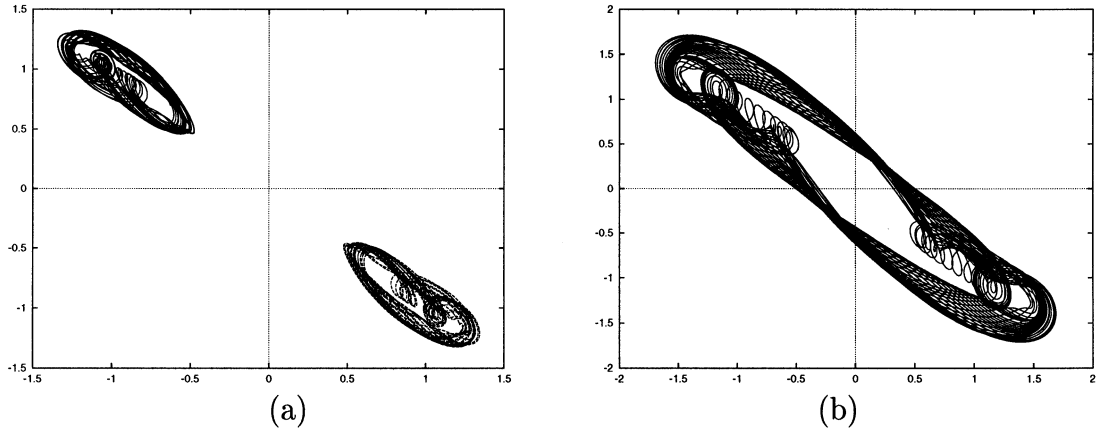

Fig. 19. Attractors of system (55) and for $N = 2$, with the set of parameters $\mathcal{B}_2^K$ given by (60) and $A = 0.088$. (a) Coexisting two-frequency tori (for the same parameters). (b) Combination of these two attractors with the formation of a double two-frequency torus.

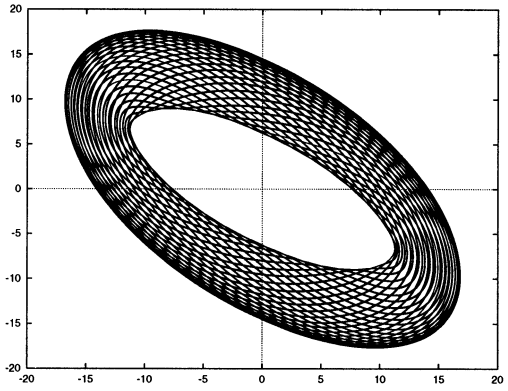

Fig. 20. Two-frequency torus attractor of system (55) for $N = 2$, with the set of parameters $\mathcal{B}_2^K$ given by (60) and $A = 5.0$.

The amplitude of the external quasi-periodic forcing A was taken as a control parameter. The following figures show coexisting two-frequency tori or strange chaotic attractors, and the corresponding x-component power spectra. With an increase of the forcing amplitude A and the number N, these coexisting attractors cling to each other giving birth to multispiral ones.

Let us remark that our computer experiments showed that for the case $N = 2$, and the set of parameters $\mathcal{B}_2^K$, upon passing through the value $A = 0.65$, the two-frequency torus (Fig. 20) subsists, the latter's radius going towards infinity as $A \to +\infty$. The same figure is obtained when $N = 4$, upon passing through the value $A = 1.1$; and when $N = 6$, upon passing through the value $A = 1.65$.

$$\begin{cases} \text{Figs. 18–21} : \mathcal{B}_2^K \text{given by (59)} \\ \text{Fig. 22} : \mathcal{B}_4^K = \mathcal{B}_2^K \cup \{s_1 = 1.11,\ s_2 = 2.06\} \\ \text{Fig. 23} : \mathcal{B}_6^K = \mathcal{B}_4^K \cup \{s_3 = 2.14,\ s_4 = 3.06\} \\ \text{Fig. 24} : \mathcal{B}_8^K = \mathcal{B}_6^K \cup \{s_5 = 5.6,\ s_6 = 6.6\} \end{cases} \tag{60}$$

6. Multibuckle in van der Pol's System

The van der Pol equation with periodic forcing is the subject of much studies. This system is given by

$$\begin{cases} \varepsilon \dfrac{dx}{dt} = y - \left(\dfrac{x^3}{3} - x \right) \\ \dfrac{dy}{dt} = -\alpha x + b \cos(t)\,, \end{cases} \tag{61}$$

where α and ε are sufficiently small and $b > 0$ (see e.g. [Itoh & Murakami, 1994] and references cited therein). The associated piecewise-linear version of (61) has been studied in [Parker & Chua, 1983]:

$$\begin{cases} \varepsilon \dfrac{dx}{dt} = y - f_2(x) \\ \dfrac{dy}{dt} = -\alpha x + b \cos(t)\,, \end{cases} \tag{62}$$

where f_2 is the nonlinear piecewise-linear function given by Eq. (2), and $m_0 = -1$ and $m_1 = 1$. In [Itoh & Murakami, 1994], the computer results for

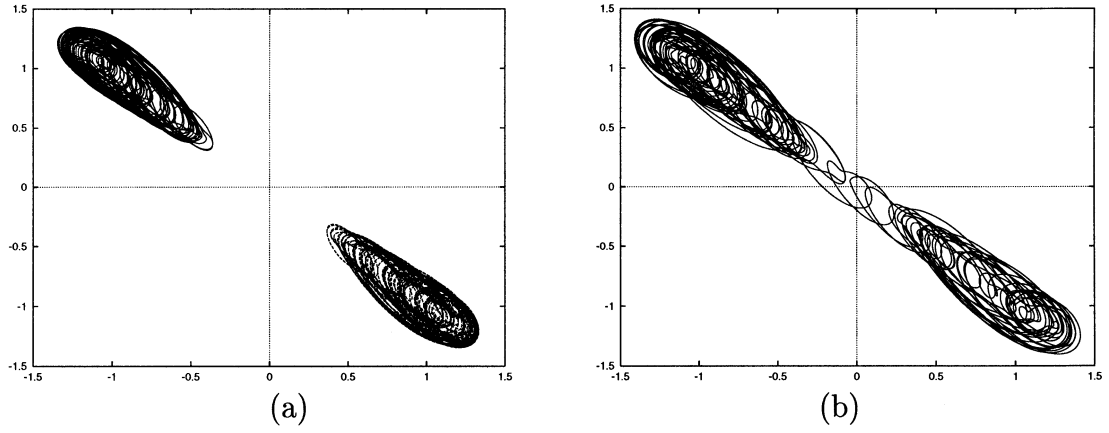

Fig. 21. (a) Coexisting chaotic attractors (for the same parameters) of system (55) for $N = 2$, with the set of parameters $\mathcal{B}_2^K$ given by (60) and $A = 0.093$. (b) Combination of these two attractors with the formation of a double one-spiral chaotic attractor when $A = 0.102$.

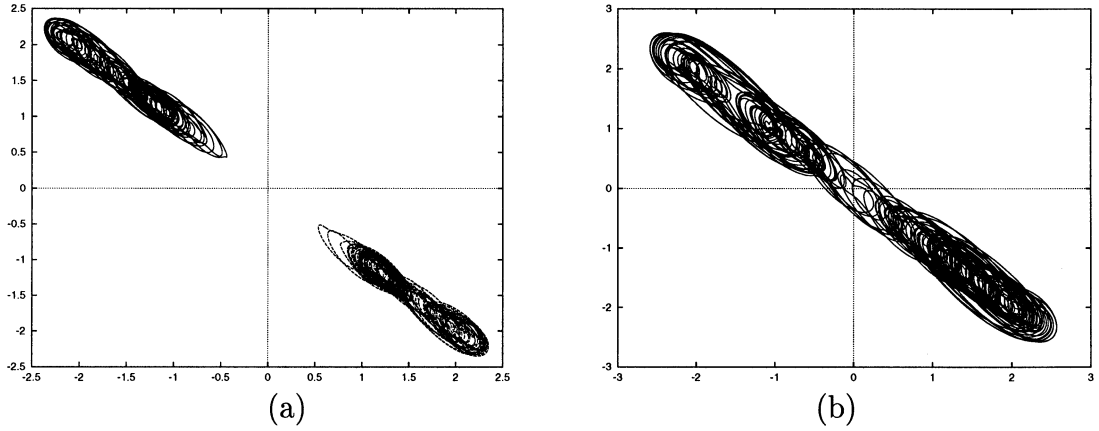

Fig. 22. (a) Coexisting two-spiral chaotic attractors (for the same parameters) for system (55) for $N = 4$, with the set of parameter $\mathcal{B}_4^K$ given by (60) and for $A = 0.095$. (b) Combination of these two attractors with the formation of a double two-spiral chaotic attractor when $A = 0.18$.

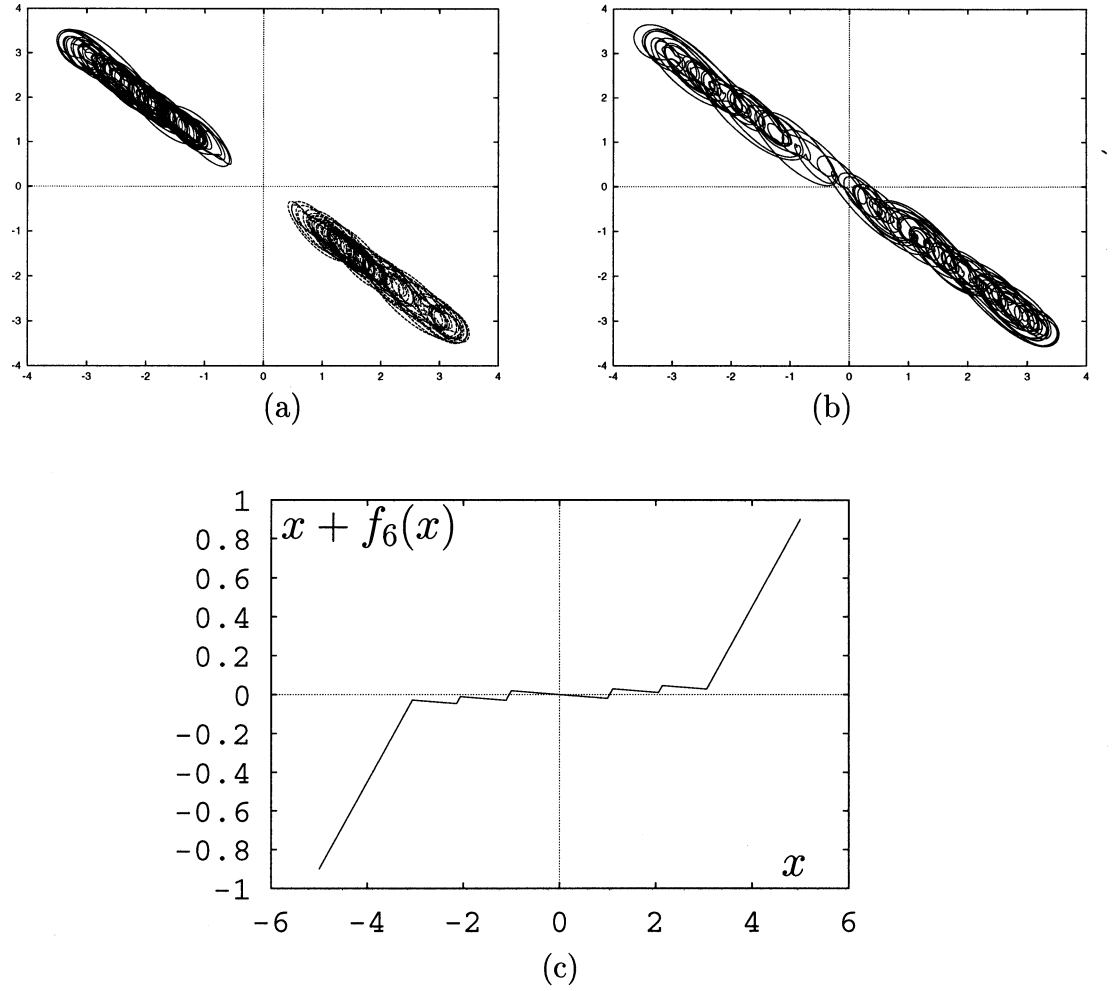

Fig. 23. (a) Coexisting three-spiral chaotic attractors (for the same parameters) for system (55) for $N = 6$, with the set of parameters $\mathcal{B}_6^K$ given by (60) and $A = 0.173$. (b) Combination of these two attractors with the formation of a double three-spiral chaotic attractor when $A = 0.18$. (c) The nonlinearity $F_6(x) = x + f_6(x)$ corresponding to the PWL characteristic which allows this attractor.

system (62) show essentially that chaotic attractors appear for:

$$\begin{cases} \alpha = \varepsilon = 0.167 \\ b = 0.59983\,. \end{cases} \tag{63}$$

The system exhibits a positive Lyapunov exponent, and the range of the parameter b corresponding to this attractor is very narrow. Furthermore, this attractor is easily destroyed by a small perturbation.

Here, we extend system (62) to obtain van der Pol strange attractors with N, $N \geq 2$, spirals (or buckles). However, we did not study whether its behavior is chaotic or not. The modified system is given by

$$\begin{cases} \varepsilon \dfrac{dx}{dt} = y - f_N(x) \\ \dfrac{dy}{dt} = -\alpha x + b\,\cos(t)\,, \end{cases} \tag{64}$$

where f_N is given by Eq. (3). This last system depends on the set of parameters:

$$\mathcal{B}_N^V = \{\alpha,\, \varepsilon,\, b\} \cup \mathcal{B}_N \subset \mathbb{R}^{2N+2}\,, \tag{65}$$

where $\mathcal{B}_N$ is given by Eq. (8), and for which we assume, as in the previous sections, that Eqs. (4) and (5) are satisfied. Furthermore, for our numerical results we set

$$\begin{aligned} &m_0 = m_{2i} = \cdots = -1.0 \\ \text{and} \quad &m_1 = m_{2i+1} = \cdots = 1.0,\ i = 1, 2, \ldots\,. \end{aligned} \tag{66}$$

Therefore, we have only to find two new parameters each time to increase the number of spirals (buckles), namely, s_1 and s_2 to find a four-spiral attractor, s_3 and s_4 to find a six-spiral attractor, and so on. The following figures (Figs. 24–27) show,

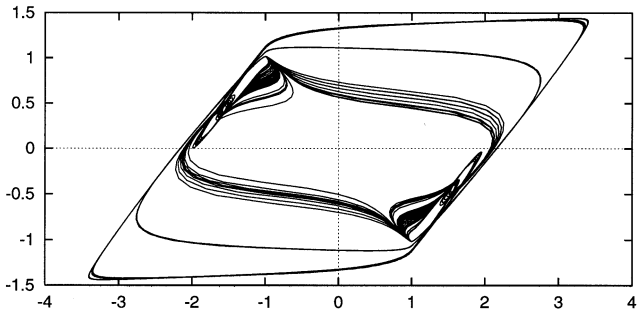

Fig. 24. Strange attractor of system (64) for $N = 2$.

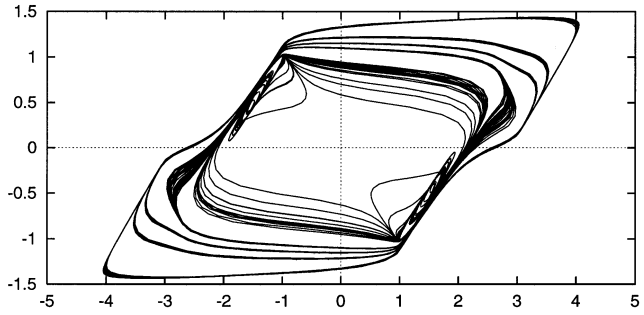

Fig. 25. Strange attractor of system (64) for $N = 4$, the same parameters as in Fig. 24 with an addition $s_1 = 2.7$, $s_2 = 3.0482$.

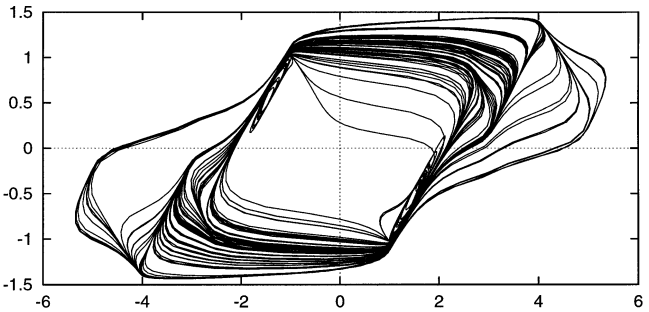

Fig. 26. Strange attractor of system (64) for $N = 6$, the same parameters as in Fig. 25 with an addition $s_3 = 4.028$, $s_4 = 4.975$.

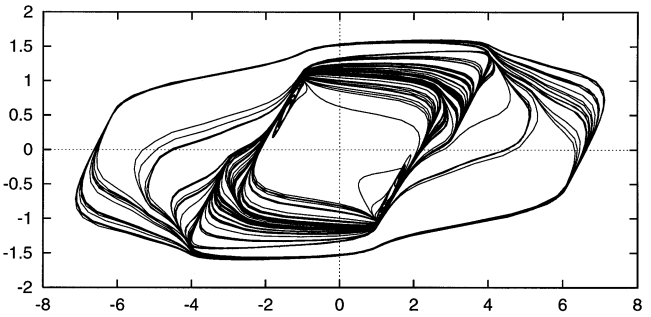

Fig. 27. Strange attractor of system (64) for $N = 8$, the same parameters as in Fig. 26 with an addition $s_5 = 5.2$, $s_6 = 6.1$.

respectively, for the parameters given by Eqs. (4), (5), (63) and (66), two-, four-, six- and eight-spiral attractors for system (64). The corresponding PWL characteristics are given in Fig. 28.

Let us also remark that for a given N, one can find strange attractors exhibiting different shapes (see Fig. 29).

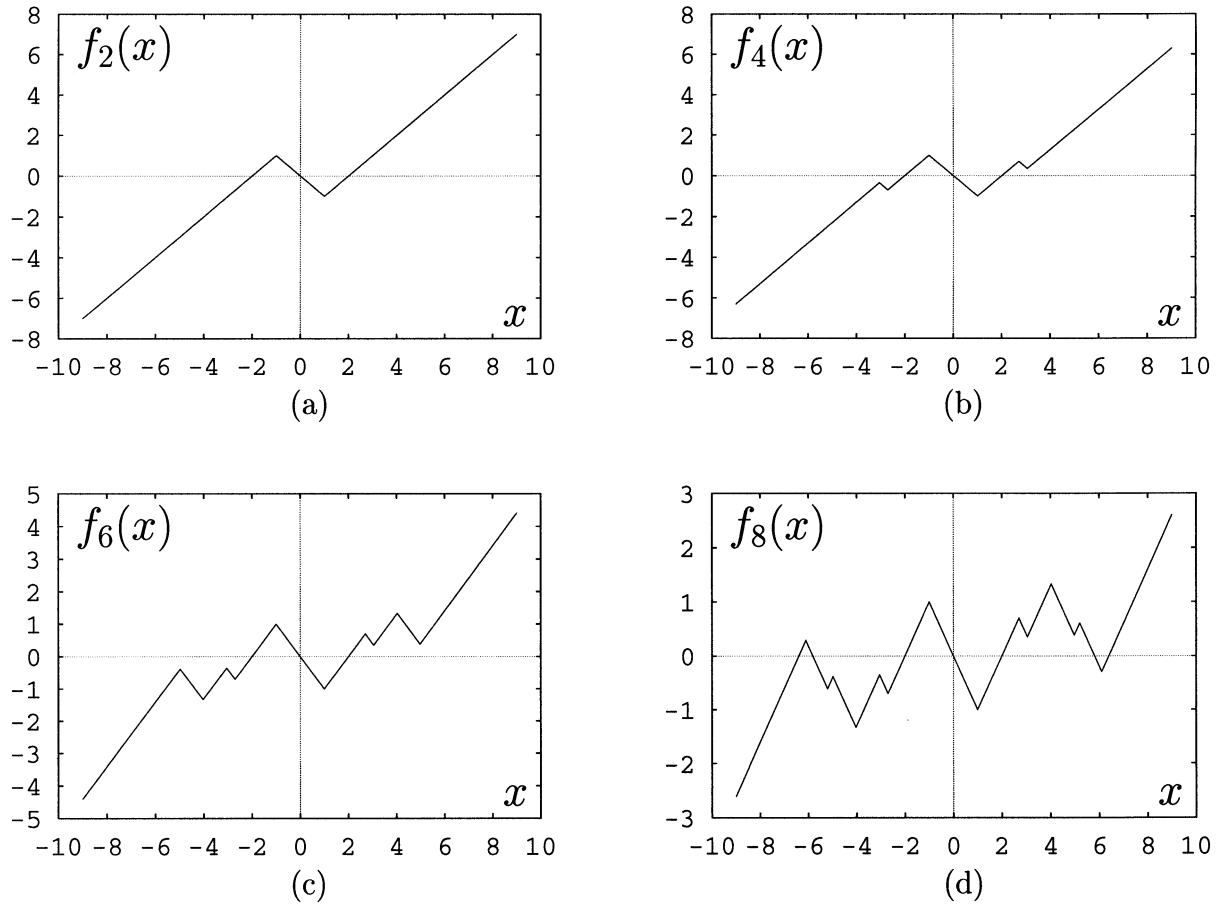

Fig. 28. Actual PWL characteristics corresponding to Figs. 24–27, respectively (from upper left, row by row).

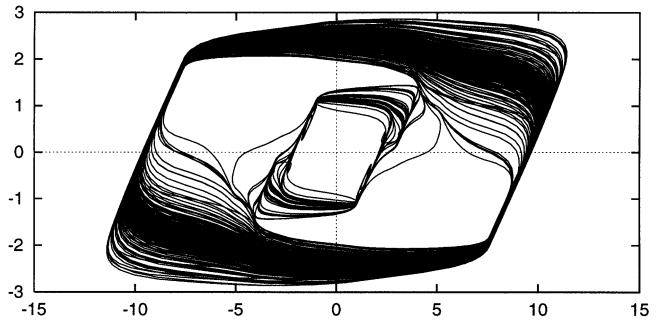

Fig. 29. Phase portrait of system (64) in the x–y plane for $N = 8$, with the same parameters as those of Fig. 26 and with $s_5 = 5.0001$ and $s_6 = 7.0$.

7. Conclusion

Various systems of differential equations having Chua's piecewise-linearity and capable of chaotic behavior have been extended, by modifying the nonlinear element, to become systems showing multispiral strange attractors. Essentially, for one of the nonautonomous systems, the evolution of the dynamics, chaos transition, and the transition towards multispiral attractors under the variation of different parameters was considered. Our computer results showed that the following conjecture is sensible:

Conjecture. *For any $N \in \mathbb{N}^*$, $N \geq 2$, there exists a nonempty set of parameters $\mathcal{B}_N$ for which each one of these systems presents strange attractors with N spirals, with the relationship,*

$$\mathcal{B}_N \subset \mathcal{B}_{N+2}\,.$$

Acknowledgments

I would like to thank both referees for their helpful suggestions and comments which allowed me to improve the quality of this paper. I also would like to thank my colleagues, Dr. C. Bourguignon and D. Hallidy of F.S.T. University of Le Havre, for

their help in editing the English text. It is a pleasure to thank Prof. A. N. Sharkovsky (guest Professor at Le Havre University in October 1998) for very helpful discussions.

References

Arena, P., Baglio, S., Fortuna, L. & Manganaro, G. [1996a] "Generation of n-double scrolls via cellular neural networks," *Int. J. Circuit Theor. Appl.* **24**, 241–252.

Arena, P., Baglio, S., Fortuna, L. & Manganaro, G. [1996b] "State controlled CNN: A new strategy for generating high complex dynamics," *IECE Trans. Fundamentals* **E79-A**, 1647–1657.

Aziz-Alaoui, M. A. [1997] "Chaos et attracteurs étranges multi-spirales dans le circuit de Chua deployé," preprint.

Aziz-Alaoui, M. A. [1998] "Nonlinear dynamics of a nonautonomous chaotic system," *Rev. Mar. Sci. Phys.* **1**, 109–125.

Brockett, R. W. [1982] "On conditions leading to chaos in feedback systems," *Proc. CDC*, pp. 932–936.

Brindley, J. & Kapitaniak, T. [1991] "Existence and characterization of strange nonchaotic attractors in nonlinear systems," *Chaos Solit. Fract.* **1**, 323–337.

Chua, L. O. [1990] "Canonical realisation of Chua's circuit family," *IEEE Trans. Circuits Syst.* **37**, 885–902.

Chua, L. O. [1992] "The genesis of Chua's circuit," *Int. J. Electron. Commun.* **46**, 250–257.

Chua L. O. [1993] "Global unfolding of Chua's circuits," *IEICE Trans. Fundamentals Electron. Commun. Comput. Sci.* **E76-A**(5), 704–734.

Chua L. O., Wu, C. W., Huang, A. & Zhong, G. Q. [1993] "A universal circuit for studying and generating chaos — Part II: Strange attractors," *IEEE Trans. Circuits Syst. I: Fundamental Theor. Appl.* **40**(10), 745–761.

Cooley, J. W. & Tukey, J. W. [1965], "An algorithm for the machine calculations of complex Fourier series," *Math. Comput.* **19**, 297–301.

Deregel, Ph. [1993] "Chua's oscillator: A zoo of attractors," in *Chua's Circuit: A Paradigm for Chaos* (World Scientific, Singapore), pp. 179–229.

Ding, M., Grebogi, O. & Ott, E. [1989] "Evolution of attractors in quasiperiodically forced systems: From quasiperiodic to strange nonchaotic to chaotic," *Phys. Rev.* **A39**, 2593–2598.

Grebogi, C., Ott, E., Pelikan, S. P. & Yorke, J. [1984] "Strange attractors that are not chaotics," *Physica* **D13**, 261–268.

Itoh, M. & Murakami, H. [1994] "Chaos and canards in the van der Pol equation with periodic forcing," *Int. J. Bifurcation and Chaos* **4**(4), 1023–1029.

Kapitaniak, T. [1997] "Strange nonchaotic trajectories on torus," *Int. J. Bifurcation and Chaos* **7**(2), 423–429.

Lacy, J. G. [1996] "A simple piecewise-linear nonautonomous circuit with chaotic behavior," *Int. J. Bifurcation and Chaos* **6**(11), 2097–2100.

Madan, R. N. (ed.) [1993] *Chua's Circuit: A Paradigm for Chaos* (World Scientific, Singapore).

Murali, K., Lakshmanan, M. & Chua, L. O. [1994] "The simplest dissipative nonautonomous chaotic circuit," *IEEE Trans. Circuits Syst.* **41**(6), 462–463.

Parker, T. S. & Chua, L. O. [1983] "A computer-assisted study of forced relaxation oscillations," *IEEE Trans. Circuits Syst.* **CAS-30**, 518–533.

Reich, H. J. [1961] *Functionnal Circuits and Oscillators* (D. van Nostrad Co., Princeton, NJ), p. 197.

Suykens, J. A. K. & Vandewalle, J. [1993] "Generation of n-double scrolls ($n = 1, 2, 3, 4, \ldots$)," *IEEE Trans. Circuits Syst.* **40**(11), 861–867.

Suykens, J. A. K., Huang, A. & Chua, L. O. [1997] "A family of n-scroll attractors from a generalized Chua's circuit," *Archiv fur Elektronik und Ubertragungstechnik* **51**(3), 131–138.

Suykens, J. A. K. & Chua, L. O. [1997] "n-double scroll hypercubes in 1D-CNNs," *Int. J. Bifurcation and Chaos* **7**(8), 1873–1885.

Testa, J., Perez, J. & Jeffries, C. [1982] "Evidence for universal chaotic behavior of a driven circuit," *Phys. Rev. Lett.* **48**, 714–717.

Ueda, Y. & Akamatsu, N. [1981] "Chaotically transitional phenomena in the forced negative-resistance oscillator," *IEEE, Trans. Circuits Syst.* **28**(3), 217–233.